Vapor pressures and isopiestic molalities of concentrated CaCl$_2$(aq), CaBr$_2$(aq), and NaCl(aq) to T = 523 K ☆

Miroslaw S. Gruszkiewicz *, John M. Simonson

Oak Ridge National Laboratory, Chemical Sciences Division, P.O. Box 2008, Building 4500S MS-6110, Oak Ridge, TN 37831-6110, USA

Abstract

The Oak Ridge National Laboratory high-temperature isopiestic apparatus was outfitted with precise pressure gauges to allow for direct vapor pressure measurements. Vapor pressures over concentrated solutions of CaCl$_2$(aq), and CaBr$_2$(aq) were measured at temperatures between (380.15 and 523.15) K in the range of water activities between 0.2 and 0.85. Isopiestic molalities were used to determine osmotic coefficients at the conditions where NaCl reference standard solutions remained undersaturated. The main goal of this work was to improve the accuracy of isopiestic comparisons based on the calcium chloride reference standard. Osmotic coefficients for CaCl$_2$(aq) and CaBr$_2$(aq) calculated from both isopiestic and direct vapor pressure results were combined with the literature data and used to build general thermodynamic models based on a variant of extended Pitzer ion-interaction equations and valid at the saturation pressure of water. While these empirical models approach the accuracy of the experimental data in a wider range of concentrations and temperatures than any previously published equations, considerable amounts of accurate data and a substantial effort are required in order to obtain a satisfactory representation using power series-based virial equations. The effect of experimental uncertainties on the accuracy of the direct vapor pressure results is discussed, including in particular the error caused by the presence in the apparatus of a small amount of CO$_2$. The substantial decrease of the solubility product of CaCO$_3$ in concentrated chloride solutions at temperatures above 423 K is a serious defect of calcium chloride as a water activity reference standard. Published by Elsevier Ltd.

Keywords: Isopiestic; Calcium chloride; Calcium bromide; Sodium chloride; Vapor pressure; Activity coefficient

1. Introduction

Aqueous CaCl$_2$ is the most common 2-1 electrolyte found in a wide range of concentrations in natural terrestrial and marine environments, in industry, agriculture and biology. While calcium chloride has been often considered a troublesome waste produced in large quantities by the Solvay soda-ash process, its uses tended to increase, and today it is even deliberately produced through the reaction of limestone with HCl or by refining of natural brine. Besides the most common high-volume uses for road deicing and dust control, CaCl$_2$ is used as a drying agent for gases and liquids, ammonia or carbon dioxide absorbent, as "high-density brines", often in combination with CaBr$_2$ and other salts, in drilling and maintaining gas and oil wells, as a cement accelerator, as a working fluid in energy conversion systems including heating and refrigeration units using solar energy, in food processing, and in other applications.

* Corresponding author. Tel.: +1 865 574 4965; fax: +1 865 574 4961.
E-mail addresses: gruszkiewicz@ornl.gov (M.S. Gruszkiewicz), simonsonjm@ornl.gov (J.M. Simonson).

Thermodynamic properties of aqueous calcium chloride are quite accurately known at $T = 298.15$ K and at elevated temperatures and moderate molalities up to about 5 mol·kg^{-1}, but uncertainties increase rapidly with increasing temperature for both very dilute and very concentrated solutions. Due in part to its much wider concentration range, CaCl$_2$(aq) is not characterized nearly as well as NaCl(aq), the representative 1-1 electrolyte. While high solubility in water, along with low price and low toxicity make calcium halides attractive in many applications, even less data exist for the more soluble CaBr$_2$. An accurate and comprehensive representation of its excess properties could justify a more widespread use of CaCl$_2$(aq) as a convenient primary isopiestic reference standard covering the range of water activities extending from saturation to below 0.2, at temperatures where sulfuric acid becomes too corrosive and even volatile. The most common isopiestic standard, NaCl(aq), reaches the state of saturation as water activity drops below about 0.75.

From the theoretical point of view it is desirable to compare and explain the behavior of various ionic solutes in wide ranges of temperature and composition. The existing interpretations have been usually limited to more or less arbitrary assignments of varying degrees of importance to a collection of several mechanisms, which often have opposite effects on macroscopic properties. These mechanisms have included creation of multiple solvation shells, electrostatic (Bjerrum) ion pairing, solvent-induced ion pairing, solvent-separated ion pairing (local hydrolysis), hydrogen-bonded-structure breaking and structure making, negative hydration, and hydrophobic hydration. Although abundant fragmentary descriptions of ion–solvent interactions have been published in the literature to rationalize various segments of the experimental database, there is no general picture of the behavior of even the simplest aqueous electrolytes, consistent enough to accommodate all the results available for anions and cations of varying sizes, and provide any predictive capabilities. The changes of solution properties with the sizes of the ions turn out to be complex and difficult to predict. For example, in the sequence MgCl$_2$(aq) ← CaCl$_2$(aq) → CaBr$_2$(aq), where, starting from CaCl$_2$, the calcium is replaced by magnesium or the chloride is replaced by bromide, the result is in both cases a decrease in vapor pressure, or an increase in the activity of the ions, for reasons that are not well understood on the molecular scale. This is reflected in the continuing difficulties in explaining the behavior of the activity coefficients of alkali metal and alkaline earth metal halides in aqueous solutions, even qualitatively [1].

Global thermodynamic models, even though they are largely empirical, provide convenient representations of thermodynamic properties for practical applications and for further research. The Pitzer ion-interaction formalism [2,3], where the short-range interactions between species are represented by virial coefficients, has been widely used since its introduction to implement such models. One of the advantages of using essentially the same model for all solutes and their mixtures is the opportunity to compare the properties and find even subtle differences in their properties. The behavior of concentrated CaCl$_2$(aq), the premier example of a 2-1 electrolyte, was found to be "anomalous" at $T = 298.15$ K by Phutela and Pitzer [4], since it deviates from the simpler pattern of MgCl$_2$(aq) starting at about 4.5 mol·kg^{-1}. While sixth and even seventh-order interaction terms (corresponding to the fifth and sixth powers of the molality) were used in equations fitting accurately the behavior of concentrated CaCl$_2$(aq) [4,5], the usual Pitzer treatment through the third order is sufficient for a satisfactory representation of the behavior of MgCl$_2$ solutions to saturation.

Parameters of Pitzer equations, valid to moderate concentrations, are available for a large number of electrolytes at $T = 298.15$ K. However, relatively few general models of any kind have been reported that extend to elevated temperatures and concentrated solutions. Although the temperature dependence of the parameters in such general models is entirely empirical, they are widely used as convenient and relatively compact representations of large sets of experimental data of varying accuracy and relevance. Among the three 2-1 type salts mentioned above, general thermodynamic models which are based on extensive collections of various experimental results and valid in a wide range of temperatures and concentrations exist for MgCl$_2$(aq) and CaCl$_2$ but not for CaBr$_2$. The general thermodynamic model for MgCl$_2$(aq) developed by Wang et al. [6] is based on experimental results at molalities extending to 25 mol·kg^{-1}, temperatures to 627 K and pressures to 100 MPa. Precise isopiestic measurements and equations for this system, valid to 4 mol·kg^{-1}, were previously reported by Holmes et al. [7,8].

Phutela and Pitzer [4] obtained a general thermodynamic model for CaCl$_2$(aq), by fitting ion-interaction equations to ambient temperature enthalpy and vapor pressure results, and using the earlier isopiestic results of Holmes et al. [7] extending to 473 K to correlate the second and third virial coefficients with temperature. Ananthaswamy and Atkinson [5] described another model valid to higher molalities (9 mol·kg^{-1}) but only to $T = 373$ K. This model is based on a variant of the ion-interaction equations extending through the sixth virial coefficient [9]. The third representation of the osmotic and activity coefficients of CaCl$_2$(aq) was published in the form of CODATA series tables [10], where the recommended values are given at molalities to 11 mol·kg^{-1} and $T = 373.15$ K. Finally, the only pressure-dependent general equations for CaCl$_2$(aq) were developed by Holmes et al. [11,12]. This accurate

model is valid for moderate concentrations (up to nearly 5 $mol \cdot kg^{-1}$) at temperatures between (273.15 and 523.15) K, and pressures to 40 MPa. It is based on a comprehensive database of available excess Gibbs free energy, calorimetric, and volumetric results, but primarily relies on the isopiestic work of Holmes and co-workers cited above.

Two further treatments have been proposed that extend the latter equations to the solubility limit of CaCl$_2$(aq) and to $T = 523.15$ K, at pure solvent saturation pressure. Pitzer and Oakes [13] used a simple empirical correlation for the osmotic coefficient with temperature-dependent parameters extending the model of Holmes *et al.* [11] to the solubility limit. More recently, Sterner *et al.* [14] described a model explicitly including speciation by combining the Pitzer's ion-interaction equations with chemical equilibria for formation of the species CaCl$^+$ and CaCl$_2^0$. They were able to adjust the 31 model parameters to obtain a good fit of the combined equations of Holmes *et al.* [11] and Pitzer and Oakes [13] at temperatures between (298.15 and 523.15) K.

The experimental data used by Pitzer and Oakes [13] above 373 K included vapor pressures over saturated solutions measured directly 125 years ago by Roozeboom [15] at temperatures up to 473 K and isopiestically by Collins and Menzies [16] (over 66 years ago) at temperatures up to 398 K. The only newer data consisted of several vapor pressures at $T = 523.15$ K reported by Ketsko *et al.* [17] and Valyashko *et al.* [18]. The reason for this scarcity of good data is that the simple isopiestic method with external weighing is increasingly more inconvenient to use as temperature increases significantly above ambient, while the accuracy required for derivation of meaningful osmotic coefficients from directly measured vapor pressures at low and moderate concentrations is difficult to achieve [19,21]. The accuracy of vapor pressures or water activities over saturated solutions may be additionally affected by the presence of multiple solid hydrates and supersaturation. Only the most careful experiments using well-designed equipment and including pressure gauges capable of high precision in a wide range of pressures can be expected to yield direct vapor pressure results of the quality that is necessary to significantly contribute to the results currently available and their extrapolations. Since both Pitzer and Oakes [13] and Sterner *et al.* [14] model parameters are based on the same sources [15–17] containing a small number of high temperature and high molality experimental data that are all subject to question, these treatments could not be considered accurate enough for support of CaCl$_2$(aq) as a primary isopiestic reference standard.

Discrepancies between different sources are significant at moderate and high concentrations even in relatively recently reported values based on critically evaluated data. At 7 $mol \cdot kg^{-1}$ and $T = 373.15$ K the discrepancy between osmotic coefficients obtained from the equations of Ananthaswamy and Atkinson [5] and the CODATA [10] treatment (2.268 and 2.417, respectively) is 6.5% – too large for a reference standard, and exceeding by a wide margin the uncertainties expected on the basis of the claimed precision of isopiestic and direct vapor pressure measurements [20,21]. Nevertheless, CaCl$_2$ has been used as an isopiestic standard at elevated temperatures at high concentrations mainly because of its convenience in comparison with H$_2$SO$_4$. For example, the model of Ananthaswamy and Atkinson [5] has been used by Grjotheim and co-workers [22–27] in a series of investigations of salt mixtures at 373 K, where calcium chloride solutions with molalities approaching 9 $mol \cdot kg^{-1}$ were used as the reference standard.

In view of the lack of accurate vapor pressures for concentrated CaCl$_2$(aq) at elevated-temperatures, and nearly no results for CaBr$_2$(aq) at temperatures other than 298.15 K, we undertook simultaneous isopiestic (relative) measurements of water activity and direct (absolute) measurements of vapor pressure over these solutions at several temperatures between (380.15 and 523.15) K. The measurements were conducted in the range of water activities between 0.85 and 0.2, approaching, but not reaching the solubility limit of CaCl$_2$. The principal goal of this work was to develop practical thermodynamic models for CaCl$_2$(aq) and CaBr$_2$(aq) that would be able to reproduce the experimental vapor pressure results in the widest possible range of temperatures and concentrations. The models described below, valid at the vapor pressure of pure solvent, are based on the extended [28] and modified Pitzer ion-interaction equations with temperature dependent coefficients.

2. Experimental

The salts used for stock solutions were the Alfa-Aesar "ultra-dry" grade, ampouled under argon. For both calcium chloride and bromide the total mass fraction of oxide, hydroxide, and water was specified as less than $5 \cdot 10^{-5}$. The mass fraction of the salt on the metals basis was specified as at least 0.9999 for the chloride and 0.99978 for the bromide. The stock solutions (approximately 3.7 $mol \cdot kg^{-1}$ and 3.3 $mol \cdot kg^{-1}$) were made by mass with air-buoyancy corrections applied, without any further verification of purity. After breaking the glass ampoules their contents were rapidly transferred to polyethylene bottles containing weighed amounts of water. Since the heats of dissolution of the anhydrous salts are significant, before adding the solids the stock bottles with water were cooled using dry ice well below freezing in order to prevent excessive temperature increases. After the solutions equilibrated with ambient

temperature, the bottles were weighed again to determine the amount of salt added.

The ORNL high-temperature isopiestic apparatus has been described previously [7,29,30]. It is the only existing facility of this type that can be used at temperatures significantly above 373.15 K. The main feature of this apparatus is its internal electromagnetic balance, which makes it possible to monitor the mass of the sample cups without interruption of the equilibrium. Other high-temperature isopiestic designs have required opening the autoclave after every equilibration in order to determine the concentrations of the samples by weighing. Removing the samples for weighing is natural at ambient temperature with very long mass transfer times. However, at elevated temperature, tight sealing of the sample cups inside the autoclave is necessary before cooling down, and corrections for the vapor space in the cups may be needed. As the temperature and the time needed to reach it both increase, while the time needed to reach thermodynamic equilibrium decreases, external weighing becomes inefficient. At temperatures above 400 K most of the time would be spent on cooling and heating the apparatus between ambient and operating temperatures. Grjotheim and co-workers [22–27] investigated a series of electrolyte mixtures using an isopiestic device of this type designed for operation at $T = 373$ K. An updated version, used for measurements at $T = 428.15$ K, was described by Brendler and Voigt [31]. More recently, Hefter et al. [32] described another one, intended for measurements to $T = 450$ K and tested at $T = 353.15$ K.

Although the isopiestic method is simple and can be very accurate, direct measurements of vapor pressure are needed to establish standard solutions in wide ranges of temperature and water activity. In order to measure vapor pressures directly and simultaneously with isopiestic ratios, precise pressure gauges were added to the ORNL isopiestic apparatus. Four Digiquartz® (Paroscientific, Inc.) pressure transmitters with pressure ranges of (0.21, 0.69, 2.1, and 6.9) MPa were connected to the isopiestic chamber. The transmitters, operating at ambient temperature through water-filled connecting lines, were placed at the level of the vapor–liquid boundary inside the apparatus, so that the water head would not exceed a few millimeters. The transmitters used nickel alloy Bourdon tubes with very small internal volumes to convert the pressure to force, and quartz crystal oscillators to convert the force to the frequency of the electrical potential, which was finally converted to a digital signal. Each pressure transmitter was also equipped with a separate quartz oscillator reading the temperature. The digitized output of this oscillator was used for temperature compensation of the pressure readings via a calibration equation residing in the transmitter memory.

The pressure transmitters were calibrated by Paroscientific using primary pressure standards traceable to the National Institute of Standards and Technology. The manufacturer specified the accuracy of gas-pressure measurement with silicone oil-filled gauges as 0.01% of their respective full-scale readings, with a resolution of 10^{-8}, however, in order to avoid problems with gas entrapment during repeated complete evacuations of the apparatus, the gauges were filled with water instead of the oil. It was estimated conservatively that under these conditions the pressure error was three times greater than nominal. Additionally, it was found that there was a hysteresis in the response of the pressure gauges to ambient temperature changes which contributed an additional uncertainty. The pressure reading shifted by a certain, limited amount depending on whether the ambient temperature of the gauge was increasing or decreasing. The reason for this hysteresis was not determined. It could have been caused by a delay between the responses of the two (pressure and temperature) quartz oscillators, or by the expansion and contraction of the fluid phases inside the bourdon tubes, where some remaining silicone oil and air might also have been trapped. Thermal insulation applied to the pressure transmitters and pressure lines mitigated this effect, but did not eliminate it. After the present measurements were completed, the temperature hysteresis was entirely eliminated by placing the pressure transducers inside a forced-convection air thermostat maintained at about $T = 312$ K and stable to ±0.1 K.

By comparing the temperature and pressure responses for all four pressure gauges, it was determined that the pressure uncertainty due to the temperature hysteresis did not exceed 0.001 MPa in the worst case. This deviation increased the expected error by a factor of 6 in the low vapor pressure range from (0.1 to 0.2) MPa, but was not significant above 0.6 MPa. Figure 1 shows the estimated absolute uncertainty in the osmotic coefficient of 2-1 electrolytes for pressures in the range between (0.1 and 4) MPa and at molalities (5, 10, 15, and 25) mol · kg^{-1}, assuming the expected accuracy of the gauges (dashed lines) and an additional error of 0.001 MPa (continuous lines). The error exceeds 0.005 MPa for the low end of the pressure range (close to 0.1 MPa) and at low molalities, but decreases quickly with increasing molality and pressure. Due to the excessive uncertainty introduced mainly by the temperature hysteresis of the pressure gauges, the osmotic coefficients obtained from directly measured vapor pressures below $T = 413$ K at low molalities were discarded. These results showed significant deviations from the isopiestic results. In order to minimize the error of pressure measurement, corrections were applied for the deviations originating from the ambient temperature drift, as determined from continuous pressure and temperature logs obtained for all four gauges.

The experimental procedure was similar to that adopted previously [7], with the exception of the loading
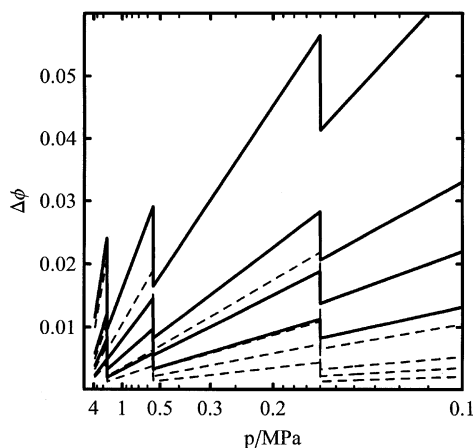
FIGURE 1. Plot of deviations of osmotic coefficient against pressure to show the propagation of the pressure measurement error for 2-1 electrolytes. The discontinuities on the curves are at the range limits where the switch between two gauge occurs. Two sets of curves are ——, for nominal pressure error only (0.0003 of the instrument range); − − −, including additionally the pressure-transmitter hysteresis error (0.001 MPa). In each set the lines correspond to (5, 10, 15, 25) mol·kg^{-1} solutions from top to bottom.

of the samples, as described below. Platinum sample cups were placed in a silver-lined stainless steel autoclave in a sample holder which could be rotated using a lever operated from the outside of the autoclave. The cups, containing no more than 10 ml of liquid rested on a large silver-clad copper block, and could be placed in turn on the pan of the electromagnetic balance. The position of the balance beam, outfitted with a platinum mirror, was detected through quartz windows by a photoresistor bridge and maintained automatically by a feedback amplifier circuit connected to the balance coil. The electric current necessary to hold the beam in the fixed position was recorded by a data acquisition system. Seven standard weights were used to determine the mass-current calibration curve for each series of weighings. A quadratic equation was used for calibration to allow for a small deviation from linearity. The calibration was made before each series of weighings. All weighings were corrected for buoyancy in steam. The temperature was controlled and measured by a platinum resistance probe secured tightly in a well drilled in the massive stainless steel lid of the autoclave. Temperature control of this location was stable to ±0.01 K over periods of several months. The autoclave was surrounded by an air bath stirred by three fans. An additional probe located lower in the air bath indicated temperature lower than the control probe by up to 1 K at $T = 523.15$ K. Considering the geometry and construction of the apparatus, the true sample temperature was estimated to always remain in the range (T_n −0.4 K, T_n +0.2 K), where T_n is the nominal temperature of 523.15 K. For $T_n = 380.15$ the true sample temperature range was estimated as T_n ± 0.1 K.

Distilled, deionized, and freshly boiled water was injected into the autoclave using a positive-displacement (chromatography) pump. During injection the supply of water was continuously sparged with helium in order to remove the remaining gases and prevent contact with the atmosphere. The time allowed to reach equilibrium after each change in water activity was at least 16 h. No indication of incomplete equilibrium was found in the cases when measurements were repeated during several days.

An automated data acquisition system sampled the pressures, temperatures, and balance currents (sample weights) simultaneously during (30 to 60) s to obtain one averaged weighing for each sample cup. Duplicate samples of each solution were placed in platinum cups in opposite locations inside the autoclave. The final result was taken as an average of 2 to 4 weighings for each of these two cups. The sample cup holder was left in varying positions for equilibration overnight and it was rotated before and during the measurements. These precautions were intended to detect and minimize the influence of possible temperature gradients inside the autoclave. The differences between the measured molalities m of duplicate samples were below ±0.003 · m for calcium chloride and less than a third of this amount for calcium bromide, sodium chloride and other samples present in the autoclave (typically ±0.0005 · m).

The main source of possible systematic molality error was probably the injection method adopted for the initial loading of the samples. The stock solutions, with molalities of 3.6947 mol·kg^{-1} for CaCl$_2$ and 3.2634 mol·kg^{-1} for CaBr$_2$ were loaded directly into the sample cups inside the autoclave using a syringe and capillary tubing (PEEK and platinum). During this operation the autoclave was maintained at $T = 380$ K with water vapor pressure inside slightly exceeding that of the injected solutions. The amounts of the salt in the cups were determined from the difference in the mass of the syringe. The solution left inside the tubing was rinsed into the cups with a small amount of water. The small differences in measured equilibrium molalities in duplicate cups could be caused by small droplets of the solution left attached to the outlet of the tubing, or incomplete rinsing of the solution remaining in dead spaces inside the connections.

Using the osmotic coefficient function $\phi(m, T)$ determined in this work one can immediately find the error $\Delta_m\phi(m, T, \Delta m)$ in the osmotic coefficient introduced by the error in molality Δm. The osmotic coefficients are calculated as ratios of two measured quantities

$$\phi_x(m_x) = F/m_x, \tag{1}$$

where m_x is the measured molality of CaX$_2$(aq), and F is a function of either the measured solvent pressure or the measured molality of the standard. For the direct method F is proportional to $-\ln a$, where a, the activity

of water, is a function of the measured vapor pressure p. For the relative isopiestic method F is the product of the reference osmotic coefficient and the measured reference molality, $F = \phi_{ref} m_{ref}$. Assuming that errors in p, and m_{ref} are zero, and the pure solvent and reference standard data used for calculation of the activity a and osmotic coefficient ϕ_{ref} are accurate, the error in the osmotic coefficient $\Delta\phi_m$ caused solely by the difference between the measured molality m_x and the true molality m_{xtrue} can be estimated as

$$\Delta_m\phi = \phi_x - \phi(m_x) = \phi(m_{xtrue})m_{xtrue}/m_x - \phi(m_x), \quad (2)$$

where ϕ_x is the osmotic coefficient obtained from the experiment (at the measured molality m_x). Assuming that $\Delta m/m = (m_x - m_{xtrue})/m_{xtrue} \ll 1$

$$\Delta_m\phi = -\Delta m[\phi(m)/m + \phi'(m)]. \quad (3)$$

Equation (3) shows that the error $\Delta_m\phi$ is zero wherever $\phi(m)$ is an inverse function of molality $\phi(m) = C/m$, where C is a constant. However, since C is proportional to $-\ln a$, and so almost always an increasing function of molality, the error $\Delta_m\phi$ nearly always has the opposite sign of the error in molality Δm (positive errors in molalities lead to negative errors in osmotic coefficients).

The uncertainty in the initial mass of the salt w_0 was estimated to be less than $\pm 0.002 \cdot w_0$ including both the error of initial loading of the sample cups and of weighing the cups on the internal electromagnetic balance to the nearest milligram. Using this value, the final model equations for the osmotic coefficient of calcium chloride described below, and equation (3), the maximum absolute error in osmotic coefficients $\Delta_m\phi$ caused solely by the error in CaX_2 molality was found to be between ± 0.003 (at $m = 3$ mol $\cdot$ kg^{-1} and $T = 523$ K) and ± 0.01 (at $m = 16$ mol $\cdot$ kg^{-1} and $T = 433$ K), in general increasing with increasing molality and decreasing with increasing temperature.

The procedure adopted in this work for loading samples differed from the simpler method used in most earlier measurements, where dry salts were placed in the sample cups. While weighing dry salts, if done rapidly, is more accurate than injecting stock solutions, it implies contact of the deliquescent solid samples with atmospheric water and carbon dioxide for at least several hours before the vessel could be closed, sealed, and evacuated. The presence of carbon dioxide leads to the formation of solid calcium carbonate and elimination of some calcium from the solution, as discussed below. Additionally, complete evacuation of the vessel containing deliquescing solids may cause loss of the salt through boiling preceding complete dryness. During this process liquid can spatter and the solid can creep out of the cups, as indicated by previous experience.

Even when samples are loaded as solutions, it would be beneficial to remove the remaining carbon dioxide adsorbed on the walls of the apparatus by flushing the autoclave with steam. This step was adopted previously [33] for isopiestic measurements of alkali metal hydroxides. However, this operation requires exposing the apparatus to the highest temperature first. Due to the properties of Teflon used for seals, leaks are likely to develop as the temperature is decreased. Complete removal of air and tight sealing at the lowest temperature is essential for vapor pressure measurements, in contrast to the isopiestic method. For this reason, and to avoid failures of the electromagnetic balance, high-temperature removal of carbon dioxide with steam was omitted.

Despite the precautions used when loading the samples and injecting water, a small amount of carbon dioxide was found to be present in the autoclave and contributed to the experimental error, in particular at the highest temperatures and molalities. This was indicated by the observed lack of repeatability of the osmotic coefficients measured at high temperature. The values obtained after reaching the maximum concentration were lower than those measured earlier for the same molalities, indicating that true molalities were below their measured values, as indicated by equation (3). The observed shifts of the osmotic coefficient ϕ were noticeable above $T = 453$ K and reached 0.035 for $CaCl_2$ and 0.015 for $CaBr_2$ at $T = 523.15$ K.

A similar "hysteresis" of the isopiestic results was observed earlier by Holmes and Mesmer [34] for alkali-metal sulfates. In this case repeated measurements at $T = 523.15$ K yielded osmotic coefficients that were higher by about 5%. No precipitate was found in the sample cups. It was concluded that the observed differences were due to the reaction of the sulfate anion with carbon dioxide desorbing from the interior surfaces of the autoclave. The bicarbonate ions produced by the reaction

$$SO_4^{2-}(aq) + CO_2(aq) + H_2O = HSO_4^-(aq) + HCO_3^-(aq) \quad (4)$$
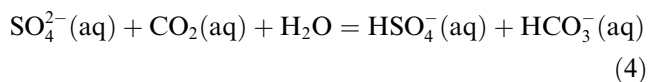
led to underestimated concentrations and overestimated osmotic coefficients. Since the difference in the osmotic coefficients seemed to exceed the amount predicted using equilibrium constant data for reaction (4), Holmes and Mesmer did not report their results at $T = 523.15$ K where this lack of repeatability was found.

We believe that carbon dioxide present inside the autoclave was also the source of "hysteresis" in the osmotic coefficients measured in this work. In our case, however, repeated measurements yielded lower osmotic coefficients, an observation consistent with the net reaction

$$CaX_2(aq) + CO_2(aq) + H_2O \rightarrow CaCO_3(cr) + 2HX(g) \quad (5)$$
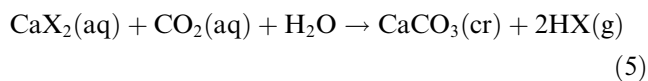
causing "disappearance" of CaX_2 from the solution and an overestimation of the true CaX_2 molality. Although the solubilities of sparingly soluble calcium compounds such as $CaCO_3$ or $Ca(OH)_2$ increase sharply with the increase of the molality of $CaCl_2$ to moderately high values such as (2 to 3) $mol \cdot kg^{-1}$, due to the formation of complex species, they are expected to start decreasing at very high $CaCl_2$ molality after reaching a maximum [35–38]. Such behavior has been observed for alkali metal salts, such as NaCl or $NaNO_3$. Since the solubility product of $CaCO_3$ (and $Ca(OH)_2$) decreases with increasing temperature, relatively small partial pressure of CO_2 can cause precipitation of $CaCO_3$ from very concentrated solutions of calcium chloride at high temperature. Due to the high reactivity of HCl or HBr, and very slow dissolution of the precipitated $CaCO_3(cr)$, reaction described by equation (5) is practically irreversible and its net result is the elimination from the solution of some calcium halide.

It was initially thought that calcium halides might be eliminated from the solutions even without the presence of carbon dioxide by the hydrolysis reaction

$$CaX_2(aq) + 2H_2O \rightarrow Ca(OH)_2(s) + 2HX(g) \qquad (6)$$

Martynova *et al.* [39] reported that noticeable decomposition of solid calcium chloride by superheated steam begins to occur between (450 and 520) K. However, hydrolysis in non-boiling liquid solutions, even very concentrated, is probably much less pronounced. The conclusive evidence for the role of CO_2 in the present work was provided by the results of X-ray diffraction analysis of the white solid precipitate found in the $CaCl_2$ and $CaBr_2$ cups after completing the measurements. The solid was found to be calcite, $CaCO_3(cr)$.

While a significant additional uncertainty due to the observed precipitation of calcite was inevitable, a correction was applied to reduce its effect. The correction accounted for the accumulation of the precipitated calcium carbonate by using the following two assumptions. First, it was assumed that the solubility product of $CaCO_3$ was only exceeded for a few highest molalities at each temperature (16 $mol \cdot kg^{-1}$ and higher for $CaCl_2$, 10 $mol \cdot kg^{-1}$ and higher for $CaBr_2$). This assumption is supported by the lack of "molality hysteresis" observed at $T = 523.15$ K at moderately high molalities (about 10 $mol \cdot kg^{-1}$ for $CaCl_2$). Second, it was assumed that the sole effect of carbon dioxide was to remove calcium halides from the solutions according to equation (5), without replacement by any other dissolved species that could affect water activity. With these assumptions, the corrected molalities of calcium halides could be calculated at each temperature by finding the approximate amounts of CaX_2 removed as calcite that were necessary to bring the osmotic coefficients obtained after reaching the highest molalities up to the original level. The relationship between the two molalities, corrected, m, and uncorrected, m' is

$$m = \frac{1 - k}{\frac{1}{m'} + k\Delta M 0.001 \ kg \cdot g^{-1}}, \qquad (7)$$

where k is the fraction of original calcium halide present in the sample cup as solid calcite for each experimental point, and ΔM is the difference between molecular masses of calcium halide and calcium carbonate, $\Delta M = 10.9$ $g \cdot mol^{-1}$ for $CaCl_2$ and $\Delta M = 99.8$ $g \cdot mol^{-1}$ for $CaBr_2$. The fractions k sufficient to cause the observed drops in the measured osmotic coefficients were found to be (0.001, 0.0018, 0.004, 0.007, 0.019, and 0.019) at (413, 433, 453, 473, 498, and 523) K, respectively, for $CaCl_2$, and were about one-third of the above values for $CaBr_2$. The fractions of the original amounts of $CaCl_2$ and $CaBr_2$ remaining in the solution at the end of the experiment were then 0.949 and 0.983. From the total amount of these salts present in the autoclave, the total amount of calcium precipitated was 1.33 mmol, equivalent to approximately 0.060 g or 30 cm^3 of carbon dioxide or 0.133 g calcite. The contribution to the uncertainty of the osmotic coefficient due to reaction (5) was estimated to reach ± 0.02 at $T = (498.15$ and $523.15)$ K and at the highest molalities (above 15 $mol \cdot kg^{-1}$), where it dominated all other sources of error. At 473 K the contribution of this error was less by approximately a factor of ten, and it was negligible at lower temperatures.

Assuming that CO_2 was physically adsorbed on the walls of the apparatus as a monolayer, the necessary surface area would be about 100 m^2. Unfortunately, the presence of a surface area of this or even greater magnitude could not be ruled out, due to some damage to the silver lining and the corrosion of stainless steel and copper present inside the autoclave. The specific surface areas of the products of iron and copper corrosion could readily exceed 10 $m^2 \cdot g^{-1}$. However, in view of the prolonged evacuation of the vessel at $T = 381$ K before starting the measurements, it seems likely that chemisorption has played a dominant role. Due to the large volume of the apparatus the pressure measurement itself was not affected by adsorption.

In summary, three sources of error were identified in addition to the random instrumental errors inherent in the measurements of temperature, pressure, and mass. These errors resulted from:

(a) the initial injection of the stock solutions – affecting molalities;
(b) temperature hysteresis of the pressure gauges – affecting pressures;
(c) precipitation of CaX_2 caused by carbon dioxide – affecting molalities.

The first of these errors was reduced by taking the molalities as averages from two samples, while the other two were mitigated by introducing corrections. The

overall maximum absolute uncertainty of a single experimental osmotic coefficient data point was estimated conservatively as ranging from no more than ±0.005 for the isopiestic results at the lower end of the temperature range to ±0.05 for direct vapor pressure measurements at the highest temperatures and molalities. The error of most osmotic coefficient values obtained in this work was less than 0.015. It is estimated that by the elimination of the above three additional sources of experimental error it will be possible in the future to decrease the uncertainty of osmotic coefficient measurement by nearly a factor of ten. Since the effect of temperature hysteresis on the pressure gauges was already eliminated, the most significant improvement can be made by careful removal of any remaining carbon dioxide from the apparatus. However, since complete elimination of carbon dioxide is in general difficult, the sensitivity to small amounts of CO_2 at high temperatures and very high molalities seems to be the most important defect of $CaCl_2(aq)$ as a universal isopiestic reference standard.

3. Results and discussion

The experimental results are given in tables 1 and 2. Table 1 contains the results based on comparisons with the sodium chloride reference solutions, while table 2 contains all the results based on direct vapor pressure measurements. All measurements described in this paper refer to the same set of samples, two of each salt. These samples were used for all measurements in a single continuous run and remained inside the isopiestic chamber over a period of several months. At the conditions where NaCl solution molalities are not given in tables 1 and 2, NaCl was completely dry. Since vapor pressure results at temperatures below $T = 413.15$ K were rejected due to low accuracy, and higher water activities were not investigated at intermediate temperatures in order to avoid repeated dissolution and drying of the NaCl, simultaneous isopiestic and direct results of high accuracy are available only at $T = (473.15, 498.15,$ and $523.15)$ K. Nevertheless, the isopiestic molalities of $CaCl_2$ and $CaBr_2$ are reported for all data points, even where a reference solution was not available for determination of the osmotic coefficients. These data provide a relationship between the two systems which is independent of the accuracy of vapor pressure measurements or reference data.

The osmotic coefficients listed in table 1 are calculated from

$$\phi_{CaX_2} = \phi_{NaCl} v_{NaCl} m_{NaCl}/(v_{CaX_2} m_{CaX_2}), \tag{8}$$

where v is the number of moles of ions produced by one mole of salt ($v = 2$ for NaCl and $v = 3$ for CaX_2), using the properties of NaCl(aq) represented by the equations

of Pitzer et al. [40]. The osmotic coefficients listed in table 2 were calculated from

$$\phi = -\Omega/(vm)\{\ln(f/f_0) + \Delta_P a(T,p,m)\}, \tag{9}$$

where Ω is the constant molality of pure water, $\Omega = 1000$ $g \cdot kg^{-1}/M_w = 55.5084$ mol $\cdot kg^{-1}$, and f and f_0 are water fugacities at the measured pressure p and at the saturated vapor pressure p_0, respectively, at the same temperature. The change in the logarithm of solvent activity as the pressure increases from p to p_0, $\Delta_P a$ (the "Poynting correction"), was treated as approximately equal to

$$\Delta_P a(T,p,m) = \overline{V}_{s,av}(m)(p_0 - p)/(RT), \tag{10}$$

where $\overline{V}_{s,av}(m)$ is the average partial molar volume of water in salt solutions in the pressure range from p to p_0 as a function of molality. Partial molar volume of the solvent $\overline{V}_s$ is related to the apparent molar volume of the solute V^ϕ by the equation

$$\overline{V}_s(m) = V_s - m^2/\Omega(\partial V^\phi/\partial m)_{p,T}, \tag{11}$$

where V_s is molar volume of pure solvent. The derivative in equation (11) was calculated using only the extended limiting law term of the Pitzer's ion-interaction treatment, so that the final expression for the partial molar volume of water applied to all the solutes was

$$\overline{V}_s = V_s - A_V|z_+z_-|vk^{1/2}m^{3/2}\Big/\Big[4\Omega\Big\{1 + b(km)^{1/2}\Big\}\Big], \tag{12}$$

where A_V is the Debye–Hückel slope for volume, $b = 1.2$ is the Pitzer parameter, and $k = \frac{1}{2}\sum v_i z_i^2$ is the ratio of the ionic strength to the molality of the salt ($k = 1$ for NaCl, $k = 3$ for CaX_2).

All the properties of water necessary for calculation of the molalities and corresponding osmotic coefficients from measured isopiestic balance current and vapor pressure data, such as liquid and vapor densities, vapor pressures, and fugacities f and f_0 were obtained from the fundamental equation of state developed by Hill [41]. Volumetric properties of the solutions used for corrections of solution masses for buoyancy and for the "Poynting correction", equations (10) to (12), were estimated and verified using several sources. For sodium chloride the equations of Archer [42] were used to obtain apparent molar volumes of the salt. This model, using Pitzer's equations including the first two virial coefficients and based on experimental data in the whole molality range, was more than adequate for this purpose. For calcium chloride, the vibrating-tube densitometry results of Oakes et al. [43], extending to $T = 523.15$ K were used to derive a simple correlation for the apparent molar volume of the salt. Since the data of Oakes et al. extended only to 6.15 mol $\cdot kg^{-1}$, their model, similar to that of Archer [42] for NaCl, could not be used for extrapolation to much higher molalities without wild

TABLE 1
Isopiestic molalities of NaCl, CaCl$_2$, and CaBr$_2$ and osmotic coefficients of CaCl$_2$ and CaBr$_2$ calculated using NaCl as the reference standard based on the model of Pitzer *et al.* [40]

m			ϕ		m			ϕ	
(mol · kg^{-1})					(mol · kg^{-1})				
NaCl	CaCl$_2$	CaBr$_2$	CaCl$_2$	CaBr$_2$	NaCl	CaCl$_2$	CaBr$_2$	CaCl$_2$	CaBr$_2$
				T = 380.15 K					
4.2210	2.3857	2.1539	1.3061	1.4467	4.4188	2.4736	2.2307	1.3317	1.4767
4.2225	2.3849	2.1550	1.3071	1.4465	4.5069	2.5128	2.2647	1.3428	1.4899
4.2226	2.3860	2.1541	1.3065	1.4471	4.6045	2.5560	2.3025	1.3551	1.5042
4.2226	2.3860	2.1549	1.3065	1.4466	4.6958	2.5970	2.3374	1.3661	1.5178
4.2747	2.4101	2.1758	1.3128	1.4542	4.6971	2.5976	2.3379	1.3663	1.5180
4.2751	2.4098	2.1744	1.3131	1.4553	4.7494	2.6241	2.3464	1.3709	1.5331
4.2754	2.4107	2.1752	1.3127	1.4549					
				T = 381.15 K					
4.7486	2.6220	2.3583	1.3703	1.5236					
				T = 383.15 K					
4.8688	2.6806	2.4059	1.3792	1.5366	4.8729	2.6832	2.4074	1.3792	1.5372
				T = 385.15 K					
4.9917	2.7398	2.4547	1.3882	1.5494					
				T = 388.15 K					
5.2207	2.8487	2.5421	1.4057	1.5752					
				T = 390.15 K					
5.3786	2.9216	2.6013	1.4181	1.5927	5.3856	2.9256	2.6041	1.4184	1.5936
				T = 393.15 K					
5.6527	2.9216	2.7033	1.4181	1.6226	6.6056	3.4421	3.0272	1.5420	1.7534
5.6572	2.9256	2.7038	1.4184	1.6238	7.1111	3.6421	3.1898	1.5947	1.8208
6.0664	3.2221	2.8463	1.4843	1.6802					
				T = 473.15 K					
4.7541	2.9485	2.4556	1.0603	1.2707	6.5889	3.8195	3.1015	1.1872	1.4586
5.5026	3.3137	2.7307	1.1156	1.3512	6.5907	3.8206	3.1028	1.1872	1.4597
6.1183	3.6029	2.9471	1.1577	1.4126	7.8987	4.4034	3.5070	1.2562	1.5743
				T = 498.15 K					
5.0339	3.2204	2.6020	0.9787	1.2090	6.8449	4.1057	3.2286	1.0808	1.3718
5.0365	3.2225	2.6024	0.9787	1.2096	8.1550	4.7112	3.6297	1.1333	1.4682
5.8080	3.6082	2.8830	1.0258	1.2814					
				T = 523.15 K					
4.7746	3.2598	2.5441	0.8522	1.0867	7.9568	4.8655	3.6151	0.9917	1.3283
5.5788	3.6872	2.8406	0.8953	1.1566	8.9524	5.3247	3.9012	1.0165	1.3809
6.4993	4.1510	3.1560	0.9399	1.2303	9.1378	5.3993	3.9514	1.0217	1.3896
6.7346	4.2717	3.2339	0.9490	1.2476					

errors. The equation chosen instead for extrapolation was

$$V_\phi = A + Bm^{r(T)}, \qquad (13)$$

where $r(T)$ was a function of temperature decreasing from about 0.5 at the boiling point of water to 0.14 at $T = 523.15$ K. Equation (13) provided a good fit to the experimental results and increased monotonically at high concentrations.

Densities of the solutions were also obtained from the empirical correlations of Sohnel and Novotny [44,45] and compared with those calculated from the V_ϕ correlation of Archer [42] for NaCl and from the extrapolation of the data of Oakes *et al.* [43] for CaCl$_2$ described above. Based on these cross-checks we believe that equations (10) to (12) provided sufficiently accurate estimates of the "Poynting correction" for all three salts and that the temperature-extrapolated density correlation given by Sohnel and Novotny for CaBr$_2$ is adequate for the buoyancy corrections. The error in the osmotic coefficients of CaX$_2$(aq) propagated from insufficient accuracy of the volumetric properties at the highest pressures and temperatures would be negligible in comparison to the experimental errors described in the previous section. However, more accurate volumetric properties of calcium halides at high temperature and molality might be needed in the future, when the errors caused by the presence of CO$_2$ are eliminated.

TABLE 2
Vapor pressures, molalities, and corresponding osmotic coefficients of CaCl$_2$ and CaBr$_2$

| p/MPa | m | | ϕ | | p/MPa | m | | ϕ | |
| | (mol · kg^{-1}) | | | | | (mol · kg^{-1}) | | | |
	CaCl$_2$	CaBr$_2$	CaCl$_2$	CaBr$_2$		CaCl$_2$	CaBr$_2$	CaCl$_2$	CaBr$_2$
				$T = 413.15$ K					
0.24608	4.2798	3.6222	1.6077	1.8996	0.17903	6.7747	5.1928	1.8658	2.4342
0.23423	4.6618	3.8961	1.6670	1.9947	0.16792	7.3184	5.4815	1.8864	2.5184
0.21562	5.3140	4.3316	1.7441	2.1396	0.15785	7.8797	5.7731	1.8948	2.5862
0.20323	5.7765	4.6233	1.7900	2.2364	0.14530	8.5200	6.0892	1.9296	2.6998
0.20321	5.7789	4.6229	1.7895	2.2370	0.13617	9.0743	6.3697	1.9422	2.7668
0.19329	6.1876	4.8591	1.8179	2.3149	0.12708	9.6915	6.6737	1.9486	2.8297
0.19256	6.1859	4.8619	1.8296	2.3278	0.11697	10.3891	7.0285	1.9636	2.9024
0.18127	6.6943	5.1488	1.8546	2.4112	0.10844	11.0762	7.3751	1.9669	2.9539
0.18115	6.6886	5.1461	1.8578	2.4146					
				$T = 423.15$ K					
0.28583	5.3987	4.3416	1.6848	2.0950					
				$T = 433.15$ K					
0.43045	4.2884	3.5666	1.4881	1.7892	0.25844	8.8267	6.1868	1.7621	2.5138
0.40015	4.9050	3.9914	1.5666	1.9251	0.23136	9.9058	6.7330	1.7727	2.6079
0.37593	5.4360	4.3309	1.6192	2.0323	0.21317	10.7017	7.1416	1.7799	2.6669
0.37582	5.4386	4.3339	1.6193	2.0319	0.19596	11.4729	7.5341	1.7937	2.7312
0.36190	5.7678	4.5348	1.6442	2.0912	0.17489	12.6244	8.1395	1.7943	2.7828
0.34280	6.2540	4.8209	1.6720	2.1690	0.15519	13.8152	8.7850	1.7976	2.8266
0.32125	6.8191	5.1375	1.7047	2.2626	0.14743	14.3782	9.0992	1.7924	2.8320
0.29643	7.5430	5.5231	1.7333	2.3670	0.13751	15.0428	9.4496	1.7979	2.8619
0.28392	7.9355	5.7224	1.7456	2.4207					
				$T = 443.15$ K					
0.55196	4.3871	3.6037	1.4395	1.7523	0.48077	5.6059	4.3987	1.5639	1.9930
				$T = 453.15$ K					
0.71409	4.2917	3.5016	1.3683	1.677	0.45140	8.6701	6.0396	1.6163	2.3199
0.67146	4.8648	3.8893	1.4296	1.788	0.43109	9.1322	6.2964	1.6249	2.3565
0.62758	5.4882	4.2836	1.4844	1.9017	0.37623	10.5365	7.0280	1.6407	2.4595
0.60700	5.7977	4.4810	1.5069	1.9495	0.32492	12.0802	7.8359	1.6503	2.5438
0.57632	6.2844	4.7650	1.5364	2.0262	0.29055	13.2773	8.4764	1.6541	2.5904
0.52983	7.0854	5.2149	1.5738	2.1381	0.25022	14.9097	9.3836	1.6551	2.6293
0.48235	8.0179	5.7122	1.5997	2.2452	0.22837	15.8932	9.9435	1.6573	2.6485
0.45151	8.6693	6.0356	1.6159	2.3207					
				$T = 473.15$ K					
1.28861[a]	2.9485	2.4556	1.0663	1.2802	0.82795	7.5248	5.3733	1.4355	2.0098
1.24737[a]	3.3137	2.7307	1.1158	1.3539	0.75604	8.4636	5.8843	1.4655	2.1073
1.21286[a]	3.6029	2.9471	1.1591	1.4169	0.69877	9.3055	6.3246	1.4828	2.1811
1.18901[a]	3.8195	3.1015	1.1823	1.4563	0.64325	10.2138	6.8073	1.4950	2.2425
1.18893[a]	3.8206	3.1028	1.1823	1.4553	0.62259	10.5743	6.9717	1.4991	2.2738
1.12274[a]	4.4034	3.5070	1.2491	1.5682	0.62238	10.5721	6.9788	1.4999	2.2707
1.08444	4.7580	3.7436	1.2817	1.6288	0.59206	11.1178	7.2916	1.5065	2.2963
1.01431	5.4365	4.1680	1.3345	1.7404	0.54251	12.1100	7.8089	1.5135	2.3444
0.95157	6.0789	4.5529	1.3761	1.8370	0.48100	13.4491	8.5564	1.5224	2.3921
0.88321	6.8518	4.9848	1.4110	1.9393	0.42457	14.9348	9.3614	1.5217	2.4267
0.88316	6.8434	4.9891	1.4129	1.9374	0.36746	16.6622	10.3168	1.5209	2.4552
0.82812	7.5055	5.3661	1.4387	2.0118	0.32549	18.0470	11.1276	1.5262	2.4740
				$T = 498.15$ K					
2.09090[a]	3.2204	2.6020	0.9913	1.2267	1.39538	7.7480	5.3821	1.2918	1.8587
2.09016[a]	3.2225	2.6024	0.9925	1.2288	1.30155	8.5002	5.8254	1.3189	1.9234
2.02318[a]	3.6082	2.8830	1.0350	1.2951	1.20058	9.4520	6.3057	1.3346	1.9991
1.93522[a]	4.1057	3.2286	1.0889	1.3843	1.10071	10.4300	6.8683	1.3550	2.0560
1.83246[a]	4.7112	3.6297	1.1420	1.4818	0.98544	11.7293	7.5508	1.3708	2.1275
1.77624	5.0487	3.8484	1.1691	1.5333	0.87652	13.1628	8.3520	1.3791	2.1714
1.72749	5.3907	4.0330	1.1818	1.5791	0.78742	14.4009	9.0549	1.3930	2.2132
1.72657	5.3873	4.0357	1.1842	1.5809	0.77515	14.5800	9.1615	1.3951	2.2181
1.72630	5.3855	4.0381	1.1851	1.5793	0.68364	16.2962	10.1069	1.3863	2.2328

(continued on next page)

TABLE 2 (continued)

| p/MPa | m | | ϕ | | p/MPa | m | | ϕ | |
| | (mol · kg^{-1}) | | | | | (mol · kg^{-1}) | | | |
	CaCl$_2$	CaBr$_2$	CaCl$_2$	CaBr$_2$		CaCl$_2$	CaBr$_2$	CaCl$_2$	CaBr$_2$
1.69140	5.5927	4.1831	1.2028	1.6075	0.54649	18.8001	11.8130	1.4162	2.2513
1.58417	6.3102	4.6084	1.2420	1.6999	0.50412	20.1277	12.3219	1.3955	2.2767
1.45121	7.2809	5.1518	1.2821	1.8110	0.44134	21.8803	13.3315	1.3941	2.2851
				$T = 523.15$ K					
3.30493[a]	3.2598	2.5441	0.8649	1.1076	2.03130	9.1443	6.0780	1.1814	1.7744
3.19908[a]	3.6872	2.8406	0.9036	1.1722	2.02630	9.1863	6.0918	1.1806	1.7772
3.08040[a]	4.1510	3.1560	0.9471	1.2448	1.90427	9.8948	6.5070	1.2030	1.8260
3.04888[a]	4.2717	3.2339	0.9587	1.2655	1.79601	10.6588	6.8963	1.2111	1.8681
2.90790[a]	4.8655	3.6151	0.9977	1.3417	1.49097	13.0355	8.2032	1.2381	1.9628
2.79800[a]	5.3247	3.9012	1.0287	1.4027	1.27887	15.0832	9.3023	1.2489	2.0198
2.77663[a]	5.3993	3.9514	1.0375	1.4164	1.20876	15.8106	9.7616	1.2546	2.0266
2.62200	6.0753	4.3535	1.0760	1.5000	0.97438	18.4621	11.4910	1.2826	2.0549
2.50494	6.6291	4.6702	1.0996	1.5589	0.92849	19.4061	11.7920	1.2650	2.0756
2.29947	7.6349	5.2432	1.1411	1.6593	0.79319	21.6372	13.0836	1.2660	2.0869
2.20803	8.1474	5.5216	1.1529	1.6986					

[a] Pressures corresponding to the NaCl molalities from table 1 at the same temperature.

The osmotic coefficients for NaCl obtained in this work from directly measured vapor pressures at $T = (473.15, 498.15,$ and $523.15)$ K are compared with the literature data in figure 2. The only results available for direct comparison in the high molality region, $m > 4.5$ mol · kg^{-1}, are those of Liu and Lindsay [46], at all three temperatures, and those and Mashovets et al. [47] at $T = (473.15$ and $523.15)$ K. At lower molalities the results of Liu and Lindsay [48], Gardner et al. [49,50], and Mashovets et al. [47] are also plotted. The lines in figure 2 represent osmotic coefficient models developed by Silvester and Pitzer [51], Pitzer et al. [40], and Archer [42], all based on Pitzer's ion-interaction approach. Examination of figure 2 shows that in the high-molality and high-temperature region all three models rely solely on the results of Liu and Lindsay [46], while in the low molality region the experimental results from all three sources show considerable deviations from the equations (up to 0.03 for Liu and Lindsay [48] and 0.05 for Mashovets et al. [47]) At $T = 473.15$ K and at molalities greater than 4.5 mol · kg^{-1}, all the experimental data, including those of Mashovets et al. and this work, are in excellent agreement. However, at $T = (498.15$ and $523.15)$ K the present results are higher than those of Liu and Lindsay [46] by about 0.01. This difference tends to increase with decreasing molality, as the slope of the present results is smaller, with quite good agreement close to saturation.

A comparison of the raw pressure data and recalculation of the literature osmotic coefficients from their vapor pressures confirmed that the differences seen in figure 2 did not originate from different sources of saturated vapor pressure data or from errors in fugacity and "Poynting correction" determinations, but instead were present in the experimental pressure and molality data.

The carbon dioxide found in our apparatus could not be the cause of the observed difference for NaCl, since any gas present in the apparatus would only cause over-estimates of water vapor pressure and underestimates of the osmotic coefficients. The temperature overestimate of about 3°, necessary to cause the observed difference, was ruled out, even though the temperature probe was not placed in direct contact with the solutions. The accuracy of pressure measurement itself should not be affected by temperature, since our pressure gauges were kept at ambient temperature. Liu and Lindsay [46] used a precise differential method using bellows and linear
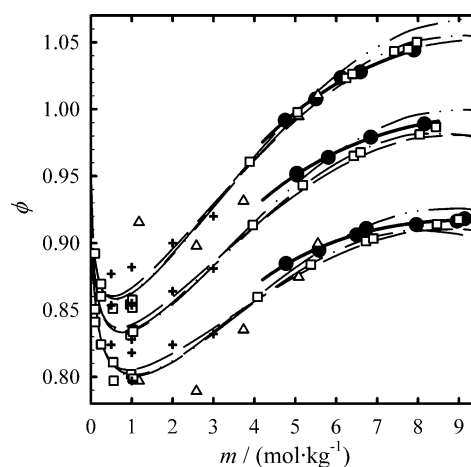

FIGURE 2. Plot of osmotic coefficients against molality for NaCl(aq) at $T = (473.15, 498.15, 523.15)$ K (osmotic coefficients decrease with increasing temperature). All symbols represent direct vapor pressure measurements. Experimental data: ●, this work; □, Liu and Lindsay [46,48]; +, Gardner et al. [49,50]; △, Mashovets et al. [47], only at $T = (473.15$ and $523.15)$ K. Equations: — —, Archer [42]; —·—, Pitzer et al. [40]; —··—, Silvester and Pitzer [51].

position transducers to measure the difference in vapor pressure between pure water and solution. Parts of this system were exposed to high temperature and had to be calibrated for the effects of temperature and pressure shifts of the null position. Given the relatively small volume of their cell, a thorough degassing was of critical importance. A careful high-pressure, high-temperature steam-cleaning operation was carried out before measurements to remove carbon dioxide and methane that formed inside their cells. Another possible source of error was the high-temperature helium calibration of the cell volume.

We conclude that it is impossible to determine the reason for the ~ 0.01 difference at $T = (498.15$ and $523.15)$ K between the present osmotic coefficients and those of Liu and Lindsay [46], especially when taking into account very good agreement at $T = 473.15$ K. While the latter results have been recognized as the most careful and accurate high-temperature direct vapor pressure measurements to date, the possibility of an error of the observed magnitude in either set of results cannot be ruled out.

3.1. Thermodynamic model for osmotic and activity coefficients

The present general models for aqueous solutions of calcium chloride and bromide are based on the modified ion-interaction (Pitzer) equations with a regular pattern of ionic-strength dependence for all virial coefficients proposed by Pitzer et al. [28]. Four virial coefficients up to the fifth (B, C, D, and E) were needed for modeling the behavior of the osmotic coefficient to very high molality, approaching the solubility limit of calcium chloride at temperatures from ambient to 525 K and above. Using the notation V_n for the nth virial coefficient, so that $B = V_2$, $C = V_3$, $D = V_4$, and $E = V_5$, the expressions for the osmotic and activity coefficients are

$$\phi = 1 - |z_+ z_-| A_\phi I^{1/2} / \left(1 + bI^{1/2}\right) + 2 \sum_{n=2}^{5} (v_1 v_2 / v)^{n/2} V_n^\phi m^{n-1},$$
(14)

$$\ln \gamma_\pm = -|z_+ z_-| A_\phi \left\{ I^{1/2} / \left(1 + bI^{1/2}\right) + 2/b \ln \left(1 + bI^{1/2}\right) \right\} + 2 \sum_{n=2}^{5} (v_1 v_2 / v)^{n/2} V_n^\gamma m^{n-1}.$$
(15)

The virial coefficients V_n^ϕ were the same functions of ionic strength and temperature defined by Pitzer et al. [28], but using only one exponential term

$$V_n^\phi = (i - 1)\{V_{n0}(T) + V_{n1}(T) \exp(-x_n)\},$$
(16)

where V_{n0} and V_{n1} are functions of only temperature, while x_n is a power function of the ionic strength

$$x_n = \alpha_n I^{(n-1)/2}.$$
(17)

The inconvenience of using more than one exponential term in equation (16) is that the optimal values for the parameters α_{nj} have to be set manually by trial and error. While this was avoided in this work by using only one exponent α_{nj} per virial coefficient, so that its optimal value could be found by using a general parameter fitting algorithm, it was necessary to replace the constant parameter α_2 associated with the second virial coefficient B^ϕ (or V_2^ϕ) by a two-parameter function of temperature

$$\alpha_2(T) = A_{\alpha 2 \, 1} / (T - A_{\alpha 2 \, 2}).$$
(18)

The temperature dependence of the exponent α_2 of the second virial coefficient was the only difference between the equations used in this work and the equations proposed by Pitzer et al. [28]. Although the substitution of equation (18) for α_{B1} is a minor modification of the temperature dependence of the osmotic and activity coefficients, it introduced some additional complexity to the equations for enthalpy and heat capacity given in the next section.

Using the relations between osmotic coefficient, the logarithm of the activity coefficient and the excess Gibbs free energy, the nth virial coefficient in equation (15) is

$$V_n^\gamma = nV_{n0}(T) + V_{n1}(T)\{g(x_n) + (n - 1) \exp(-x_n)\}$$
(19)

with

$$g(x_n) = 2/x_n^2\{1 - (1 + x_n) \exp(-x_n)\}, \quad g(0) = 1.$$
(20)

The parameters $V_{n0}(T)$ and $V_{n1}(T)$ were expressed as linear combinations of at most six terms

$$V_{nj} = A_{nj \, 1} + A_{nj \, 2} T^{-1} + A_{nj \, 3}(650 - T)^{-1} + A_{nj \, 4} T + A_{nj \, 5} T^2 + A_{nj \, 6} T^{-2}.$$
(21)

To determine the parameters $A_{\alpha 2 \, 1}$, $A_{\alpha 2 \, 2}$, α_3, α_4, α_5 and $A_{nj \, i}$, where $n = 2 \ldots 5$, $j = 0$ or 1, and $i = 1 \ldots 6$, a least-squares procedure was used to fit equations (14) to (21) to the database consisting of about one thousand osmotic coefficient data points, and a few activity coefficient data points. The database consisted of the present results listed in tables 1 and 2 together with earlier osmotic and activity coefficient data found in the literature. All of the available data were examined, and varying weights were assigned to individual data sets depending on their estimated accuracy and agreement with key datasets.

It was found that the available experimental data were not sufficient for finding a set of parameters A_{ij} producing a well-behaved function $\phi(m, T)$ extending beyond the region where experimental results were available, so that a limited extrapolation or even satisfactory interpolation could be expected. This is not surprising, considering that the universal power-series-based equations (14) to (21) do not carry any physical information

about the system as a function of molality or temperature, besides the limiting behavior of very dilute solutions. Nearly all the information on thermodynamic behavior is contained in the optimal sets of adjustable parameters. While the number of adjustable parameters, determined by the functional form of the equations and the complexity of the system, cannot be reduced, it is possible to utilize our knowledge of thermodynamic behavior of similar systems to enforce the expected behavior of $\phi(m, T)$ at molalities and temperatures extending beyond the range of reliable experimental data. This was achieved by adding to the experimental database a synthetic data set representing the expected extrapolated behavior. Although the resulting model parameters are reasonably well defined by the extended experimental and synthetic database, they are necessarily "overfitted" with respect to the experimental data alone, and since their uncertainties are meaningless, they are not reported here. Other than abandoning the development of such general models altogether, the alternative choices were either to obtain more experimental data, or to develop a thermodynamic model incorporat-

ing some fundamental elements of the behavior of concentrated aqueous solutions. While these goals might be worth pursuing in the future, the empirical models described here fulfill the primary objective of this work. They provide a practical means for reproducing numerically the best estimates for the osmotic coefficients of aqueous solutions calcium chloride and calcium bromide with the accuracy approaching that of experimental data, in the widest possible range of temperatures and molalities.

The parameters in equations (16) to (20) for $CaCl_2(aq)$ and $CaBr_2(aq)$ are given in table 3. Osmotic coefficients of $CaCl_2(aq)$ and of $CaBr_2(aq)$ are shown in figures 3 and 4, respectively. The lines represent the equations plotted as isotherms from $T = 273.15$ K (top) to $T = 623.15$ K (bottom), every 25 K. The ranges of temperature and molality where measurements were made, roughly contained between water activities of 0.2 and 0.8, are indicated by the symbols representing most of the new experimental results. The bold continuous line in figure 3 is the locus of the saturated solutions, essentially in agreement with the CODATA review [10]. At temperatures above 500 K, however, the uncertainty of the solubility increases significantly. The solubility results of Valyashko *et al.* [18] (broken line) are significantly higher that these recommended values. Due to the difficulties inherent in determination of solubility, and consequently a large uncertainty of high-temperature vapor

TABLE 3
Parameters of equations (16), (17), and (20)

	CaCl$_2$	CaBr$_2$
$A_{\alpha2\ 1}$	390.0	475.0
$A_{\alpha2\ 2}$	190.0	178.0
α_3	0.600	0.550
α_4	0.075	0.058
α_5	0.029	0.020
$A_{20\ 1}$	0.721737030	2.42139782
$A_{20\ 2}$	212.464638	0.0
$A_{20\ 3}$	0.418636550	0.208233793
$A_{20\ 4}$	-0.00344719151	-0.00721597004
$A_{20\ 5}$	$3.17878483 \cdot 10^{-6}$	$6.35945998 \cdot 10^{-6}$
$A_{21\ 1}$	1.63282102	1.79553223
$A_{21\ 3}$	39.5766049376	0.0
$A_{21\ 4}$	0.0	$6.199603005 \cdot 10^{-4}$
$A_{30\ 1}$	0.0181265080	-0.0198238648
$A_{30\ 2}$	-17.6613361	-5.585540455
$A_{30\ 4}$	$5.87061823 \cdot 10^{-5}$	$7.12836328 \cdot 10^{-5}$
$A_{30\ 5}$	$-7.44440747 \cdot 10^{-8}$	$-7.045825025 \cdot 10^{-8}$
$A_{31\ 1}$	1.050242670479	-0.0444796144
$A_{31\ 4}$	-0.00180877670	0.0
$A_{31\ 6}$	$-7.43937796 \cdot 10^{4}$	$-3.29046152 \cdot 10^{4}$
$A_{40\ 1}$	-0.00216247849	$1.142604645 \cdot 10^{-4}$
$A_{40\ 2}$	0.733081559	0.0680402852
$A_{40\ 4}$	$1.62174006 \cdot 10^{-6}$	0.0
$A_{41\ 1}$	0.205227852	0.437976179
$A_{41\ 2}$	-28.7506035	-146.486424
$A_{41\ 4}$	$-2.47122732 \cdot 10^{-4}$	$-3.89325593 \cdot 10^{-4}$
$A_{41\ 6}$	-5551.23750	$1.22648510 \cdot 10^{4}$
$A_{50\ 1}$	$9.10253049 \cdot 10^{-6}$	$-1.47824162 \cdot 10^{-6}$
$A_{50\ 2}$	0.0	$-3.07209240 \cdot 10^{-4}$
$A_{50\ 4}$	$-9.27266902 \cdot 10^{-9}$	0.0
$A_{50\ 6}$	-1.331311225	0.0
$A_{51\ 1}$	0.0118620021	0.004093673345
$A_{51\ 2}$	-10.9172865	-4.38084199
$A_{51\ 6}$	2362.70693	1108.17571

The parameters that are zero for both CaCl$_2$ and CaBr$_2$ are omitted.
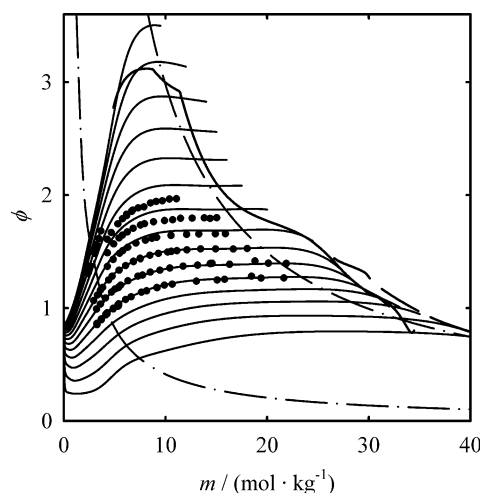
FIGURE 3. Plot of osmotic coefficients against molality for $CaCl_2(aq)$ at $T = (273.15, 298.15, 323.15, 348.15, 373.15, 398.15, 423.15, 448.15, 473.15, 498.15, 523.15, 548.15, 573.15, 598.15, 623.15)$ K. The isotherms were calculated from equation (14) and the following equations with parameters from table 3. Most of the experimental results of this work were also plotted as symbols to indicate the temperature and molality ranges. The bold continuous line represents saturated solutions based on the review of Smith-Magovan *et al.* [10] (see text). The dashed bold line represents the solubility limit based on the measurements of Valyashko *et al.* [18]. The dot-dashed lines show the range of water activity between 0.2 (bottom line) and 0.8 (top line) where most of the measurements were made.
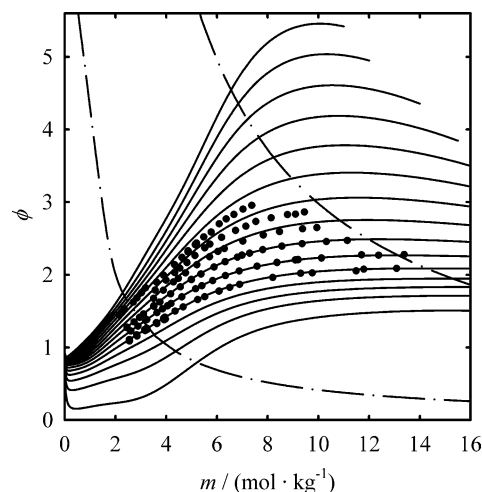
FIGURE 4. Plot of osmotic coefficients against molality for CaBr$_2$(aq) at T = (273.15, 298.15, 323.15, 348.15, 373.15, 398.15, 423.15, 448.15, 473.15, 498.15, 523.15, 548.15, 573.15, 598.15, 623.15) K. The isotherms were calculated from equation (14) and the following equations with parameters from table 3. Most of the experimental results of this work were also plotted as symbols to indicate the temperature and molality ranges. The dot-dashed lines show the range of water activity between 0.2 (bottom line) and 0.8 (top line) where most of the measurements were made.

pressure data at saturation, it is not certain whether osmotic coefficient isotherms reach a maximum before saturation.

For reference and for verification of numerical calculations, tables 4 to 7 lists the calculated values of osmotic and activity coefficients at several even temperatures and molalities almost to saturation. The number of digits listed in these tables is not intended to be an indication of accuracy. Note that the uncertainty increases rapidly at high temperature as the molality is approaching saturation beyond the limit of the present experimental data, where neither vapor pressure nor solubility data are accurate.

3.2. Contributions of previous data to the model

While the exact values of the weights assigned to each experimental data set are arbitrary and not relevant in this work for the reasons described above, we find it useful to discuss in general terms the relative contributions of the data sets included in the experimental database, and their agreement with the present results and other key data.

TABLE 4
Osmotic coefficients ϕ of CaCl$_2$(aq) calculated using equation (14) and the parameters from table 3

m (mol · kg^{-1})	T/K = 323.15	T/K = 373.15	T/K = 423.15	T/K = 473.15	T/K = 523.15	T/K = 573.15
0.01	0.9043	0.8904	0.8714	0.8458	0.8097	0.7516
0.1	0.8468	0.8239	0.7884	0.7377	0.6641	0.5465
0.2	0.8478	0.8218	0.7831	0.7269	0.6445	0.5129
0.3	0.8584	0.8275	0.7853	0.7255	0.6382	0.5002
0.4	0.8737	0.8369	0.7899	0.7259	0.6344	0.4919
0.5	0.8926	0.8494	0.7965	0.7276	0.6317	0.4851
0.6	0.9146	0.8650	0.8055	0.7310	0.6303	0.4796
0.8	0.9658	0.9042	0.8306	0.7436	0.6322	0.4726
1.0	1.0240	0.9517	0.8640	0.7636	0.6407	0.4715
1.5	1.1827	1.0869	0.9666	0.8340	0.6821	0.4875
2.0	1.3478	1.2249	1.0742	0.9119	0.7336	0.5155
3.0	1.6946	1.5061	1.2895	1.0667	0.8388	0.5822
4.0	2.0605	1.7890	1.4958	1.2110	0.9407	0.6619
5.0	2.3987	2.0124	1.6415	1.3092	1.0180	0.7410
6.0	2.6426	2.1585	1.7316	1.3714	1.0734	0.8059
7.0	2.7812	2.2460	1.7914	1.4184	1.1179	0.8553
8.0	2.8462	2.2944	1.8316	1.4555	1.1550	0.8938
9.0	2.8698	2.3179	1.8563	1.4826	1.1848	0.9254
10.0	2.8721	2.3261	1.8692	1.5008	1.2079	0.9520
11.0	2.8644	2.3258	1.8742	1.5119	1.2253	0.9743
12.0		2.3217	1.8745	1.5179	1.2378	0.9929
14.0			1.8712	1.5218	1.2530	1.0202
16.0			1.8719	1.5235	1.2607	1.0372
18.0				1.5278	1.2660	1.0473
20.0				1.5328	1.2712	1.0531
22.0				1.5294	1.2754	1.0566
24.0				1.5017	1.2744	1.0585
26.0					1.2604	1.0584
28.0						1.0542
30.0						1.0428

TABLE 5
Natural logarithm of the mean activity coefficients of CaCl$_2$(aq) ln$\gamma_\pm$ calculated using equation (15) and the parameters from table 3

m	$T/K = 323.15$	$T/K = 373.15$	$T/K = 423.15$	$T/K = 473.15$	$T/K = 523.15$	$T/K = 573.15$
(mol · kg^{-1})						
0.01	−0.3293	−0.3745	−0.4359	−0.5181	−0.6349	−0.8234
0.1	−0.6824	−0.7804	−0.9222	−1.1180	−1.3982	−1.8478
0.2	−0.7882	−0.9060	−1.0767	−1.3150	−1.6583	−2.2085
0.3	−0.8375	−0.9716	−1.1622	−1.4276	−1.8101	−2.4213
0.4	−0.8609	−1.0107	−1.2188	−1.5061	−1.9185	−2.5746
0.5	−0.8682	−1.0332	−1.2583	−1.5654	−2.0031	−2.6955
0.6	−0.8639	−1.0438	−1.2857	−1.6114	−2.0719	−2.7955
0.8	−0.8304	−1.0383	−1.3133	−1.6747	−2.1762	−2.9533
1.0	−0.7738	−1.0072	−1.3143	−1.7098	−2.2490	−3.0723
1.5	−0.5758	−0.8664	−1.2480	−1.7227	−2.3461	−3.2682
2.0	−0.3355	−0.6845	−1.1352	−1.6819	−2.3791	−3.3839
3.0	0.2170	−0.2596	−0.8495	−1.5335	−2.3622	−3.5015
4.0	0.8326	0.2084	−0.5307	−1.3495	−2.2922	−3.5313
5.0	1.4451	0.6333	−0.2574	−1.1928	−2.2194	−3.5190
6.0	1.9673	0.9779	−0.0418	−1.0684	−2.1556	−3.4954
7.0	2.3706	1.2512	0.1356	−0.9604	−2.0963	−3.4720
8.0	2.6783	1.4696	0.2843	−0.8650	−2.0410	−3.4501
9.0	2.9210	1.6471	0.4085	−0.7825	−1.9911	−3.4292
10.0	3.1206	1.7946	0.5124	−0.7125	−1.9473	−3.4091
11.0	3.2910	1.9207	0.6005	−0.6531	−1.9093	−3.3902
12.0		2.0319	0.6769	−0.6023	−1.8765	−3.3730
14.0			0.8082	−0.5182	−1.8234	−3.3446
16.0			0.9252	−0.4467	−1.7814	−3.3237
18.0				−0.3805	−1.7451	−3.3086
20.0				−0.3196	−1.7116	−3.2975
22.0				−0.2723	−1.6813	−3.2888
24.0				−0.2548	−1.6584	−3.2818
26.0					−1.6508	−3.2773
28.0						−3.2772
30.0						−3.2852

TABLE 6
Osmotic coefficients ϕ of CaBr$_2$(aq) calculated using equation (14) and the parameters from table 3

m	$T/K = 323.15$	$T/K = 373.15$	$T/K = 423.15$	$T/K = 473.15$	$T/K = 523.15$	$T/K = 573.15$
(mol · kg^{-1})						
0.01	0.9073	0.8939	0.8752	0.8498	0.8133	0.7537
0.1	0.8612	0.8395	0.8065	0.7584	0.6857	0.5609
0.2	0.8703	0.8429	0.8074	0.7570	0.6792	0.5404
0.3	0.8871	0.8520	0.8132	0.7623	0.6845	0.5419
0.4	0.9077	0.8641	0.8209	0.7689	0.6917	0.5486
0.5	0.9314	0.8794	0.8310	0.7770	0.7000	0.5571
0.6	0.9580	0.8984	0.8443	0.7873	0.7097	0.5665
0.8	1.0192	0.9469	0.8811	0.8161	0.7341	0.5882
1.0	1.0888	1.0077	0.9309	0.8560	0.7660	0.6134
1.5	1.2822	1.1905	1.0926	0.9899	0.8698	0.6854
2.0	1.4883	1.3877	1.2730	1.1421	0.9855	0.7589
3.0	1.9447	1.7921	1.6265	1.4338	1.2074	0.9084
4.0	2.4668	2.2245	1.9727	1.7057	1.4240	1.0939
5.0	3.0436	2.6682	2.2979	1.9466	1.6228	1.2956
6.0	3.6109	3.0679	2.5669	2.1332	1.7770	1.4669
7.0	4.0651	3.3748	2.7654	2.2661	1.8859	1.5918
8.0	4.3637	3.5798	2.9005	2.3579	1.9614	1.6773
9.0	4.5291	3.7019	2.9862	2.4193	2.0128	1.7344
10.0	4.5999	3.7640	3.0352	2.4578	2.0467	1.7721
11.0	4.6043	3.7831	3.0572	2.4790	2.0679	1.7968
12.0	4.5592	3.7698	3.0588	2.4874	2.0799	1.8127
14.0		3.6706	3.0182	2.4788	2.0877	1.8285
16.0			2.9373	2.4503	2.0845	1.8313
18.0			2.8258	2.4079	2.0732	1.8213

TABLE 7
Natural logarithm of the mean activity coefficients of CaBr$_2$(aq) ln$\gamma_\pm$ calculated using equation (15) and the parameters from table 3

m (mol · kg^{-1})	T/K = 323.15	T/K = 373.15	T/K = 423.15	T/K = 473.15	T/K = 523.15	T/K = 573.15
0.01	−0.3225	−0.3669	−0.4277	−0.5098	−0.6272	−0.8189
0.1	−0.6471	−0.7410	−0.8774	−1.0685	−1.3486	−1.8163
0.2	−0.7322	−0.8484	−1.0110	−1.2387	−1.5764	−2.1501
0.3	−0.7649	−0.9014	−1.0822	−1.3310	−1.7003	−2.3348
0.4	−0.7740	−0.9303	−1.1273	−1.3919	−1.7829	−2.4591
0.5	−0.7685	−0.9437	−1.1561	−1.4345	−1.8425	−2.5505
0.6	−0.7521	−0.9451	−1.1725	−1.4639	−1.8867	−2.6209
0.8	−0.6948	−0.9194	−1.1758	−1.4927	−1.9427	−2.7211
1.0	−0.6136	−0.8642	−1.1474	−1.4898	−1.9667	−2.7852
1.5	−0.3482	−0.6448	−0.9844	−1.3901	−1.9391	−2.8566
2.0	−0.0330	−0.3658	−0.7528	−1.2201	−1.8450	−2.8635
3.0	0.7054	0.2717	−0.2212	−0.8147	−1.5866	−2.7841
4.0	1.5692	0.9904	0.3528	−0.3804	−1.2806	−2.6005
5.0	2.5346	1.7553	0.9307	0.0448	−0.9652	−2.3560
6.0	3.5256	2.4955	1.4611	0.4213	−0.6831	−2.1150
7.0	4.4184	3.1456	1.9170	0.7394	−0.4457	−1.9081
8.0	5.1474	3.6822	2.2973	1.0067	−0.2467	−1.7376
9.0	5.7197	4.1159	2.6121	1.2319	−0.0788	−1.5973
10.0	6.1666	4.4663	2.8733	1.4221	0.0637	−1.4801
11.0	6.5148	4.7500	3.0905	1.5834	0.1857	−1.3806
12.0	6.7817	4.9785	3.2713	1.7209	0.2912	−1.2946
14.0		5.2999	3.5456	1.9413	0.4663	−1.1521
16.0			3.7293	2.1085	0.6082	−1.0384
18.0			3.8398	2.2346	0.7240	−0.9509

The only activity coefficient data included were those of McLeod and Gordon [52] and Mussini and Pagella [53], both as calculated by Ananthaswamy and Atkinson [5] from the original EMF results. Since both data sets are at molalities (less than 0.1 mol · kg^{-1}) and T = (288.15 to 343.15) K, which are well below the current results, they were used with large weights. The deviation of these results from the current model is increasingly negative with increasing molality and temperature.

The osmotic coefficients at T = 298.15 K, tabulated by Rard and Clegg [21] were used as the basis for the new model at low temperature. The smoothed values listed by Rard and Clegg were generated using a rather complex speciation model using 22 adjustable parameters (four of which were set to zero) regressed from a database of critically assessed experimental results obtained by various methods. The deviation of the present model at T = 298.15 K from the values recommended by Rard and Clegg [21] is compared in figure 5 with the corresponding deviation from the same values of the T = 298.15 K equation of Pitzer et al. [28], and the temperature and pressure-dependent equation of Holmes et al. [11]. The average absolute deviation of the present model in the range from zero to 11 mol · kg^{-1} is less than 0.005, but it reaches 0.013 at moderately high concentration. The deviation of the nine-term equation of Pitzer et al. is less than 0.004 over the whole concentration range, reaching 0.006 only at a molality close to 11 mol · kg^{-1}. While the best measurements of osmotic

coefficients in the moderately concentrated region are probably accurate to ±0.003, they can only be identified by evaluation of large databases. Different assignment of weights to various datasets can cause larger differences, and indeed, some earlier equations [4,54] for Ca-Cl$_2$(aq) at T = 298.15 K deviate from the values of Rard and Clegg by more than 0.01. Taking into account the wide temperature and molality range of the present model using 32 adjustable parameters versus 14 for the equation of Pitzer et al. [28], which is valid only at T = 298.15 K to 11 mol · kg^{-1}, this sacrifice of accuracy
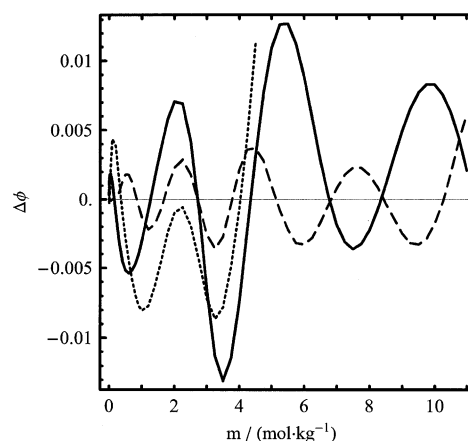

FIGURE 5. Plot of deviations of osmotic coefficients at T = 298.15 K from the equation of Rard and Clegg [21] against molality. ——, current temperature-dependent model; – – –, the T = 298.15 K equation of Pitzer et al. [28]; - - - - - - -, the model of Holmes et al. [11].

at low temperature seems reasonable. For ultimate accuracy at $T = 298.15$ K, the values of Rard and Clegg [21] or the equation of Pitzer et al. [28] can be used.

Other low-temperature data sources included freezing-point data measurements of Gibbard and Fong [55] for freezing-point depressions reaching 4 K (0.0275 mol $\cdot$ kg^{-1} to 0.73 mol $\cdot$ kg^{-1} CaCl$_2$) and of Oakes et al. [56] for freezing-point depressions reaching 50 K (4.0 mol $\cdot$ kg^{-1} CaCl$_2$), and the isopiestic results using sulfuric acid as the reference standard at $T = 288.15$ K of Childs and Platford [57] and at $T = 273.15$ K of Platford [58] at molalities from (0.5 to 7) mol $\cdot$ kg^{-1}. While the accuracy of the model decreases significantly with temperature decreasing below 298.15 K, since the freezing point data for very low temperature are much less accurate due to the approximations necessary for calculation of the osmotic coefficients, and no results are available for dilute solutions, a qualitatively reasonable behavior of the model was achieved at temperatures significantly below 273 K.

At temperature to 523.15 K and at molality to 4 mol $\cdot$ kg^{-1} the present model for CaCl$_2$ agrees well with the equations of Holmes et al. [11]. Essentially, the entire set of osmotic coefficient data they used to parameterize their equations was also included in the present database. Of crucial significance among those were their own experimental isopiestic results [7,11] using NaCl as the reference standard in the temperature range $T = (382$ to $524)$ K at molalities reaching 4.8 mol $\cdot$ kg^{-1} CaCl$_2$ at the highest temperature. It was somewhat surprising that the several sets of data reported between room temperature and the lower limit of both the present data and the data of Holmes et al. (about 380 K), at high molalities exceeding 4.5 mol $\cdot$ kg^{-1}, were in substantial disagreement with each other. This was the main reason why, besides the interpolation between the present experimental results and accurate data at $T = 298.15$ K and below, we decided to rely upon the older data for saturated solutions [15,16,59]. In this region only the two results of Bechtold and Newton [60], recalculated by Anathaswamy and Atkinson [5] for 7 mol $\cdot$ kg^{-1} CaCl$_2$ at $T = (308.15$ and $318)$ K, were found to be consistent with all the key results.

A number of other experimental datasets [61–72] were used in part, used with very small weights, or not used at all in the final regression, due to either significant deviations from the data described above or to insufficient precision. Among these, the high temperature vapor pressure results, in particular those above 523.15 K to moderate concentrations were in general not precise enough to quantitatively improve the extrapolation of the present results combined with the model of Holmes et al. [11]. The measurements of Wood et al. [65] in the range $T = (473.15$ to $623.15)$ K were at least as uncertain as the older high-temperature work [66]. The osmotic coefficients determined from the bubble

pressures measured by Crovetto et al. [67] at $T = 623.15$ K did not agree with these two earlier sources or with the extrapolation of the data at $T = 523.15$ K and lower temperatures. Taking into account their precision, the high-temperature, high-molality results of Ketsko et al. [17] and Valyashko et al. [18] reaching $T = 673.15$ K at molalities exceeding 50 mol $\cdot$ kg^{-1}, were in reasonably good general agreement with the present model.

In contrast to the high-temperature results discussed above, the osmotic coefficients reported by Jakli and van Hook [68], who used a precise differential pressure apparatus to measure solvent vapor pressures in the temperature range $T = (295$ to $374)$ K, apparently deviate from the present equation due primarily to systematic errors. Jakli and van Hook applied a correction for unknown water content in their calcium chloride and noted a remaining $0.05 \cdot \phi$ deviation from accepted values of their 7.9 mol $\cdot$ kg^{-1} osmotic coefficient results at $T = 298.15$ K. While direct comparison with the present data is not possible, it can be established with near certainty that the high-molality osmotic coefficients of Jakli and van Hook are significantly underestimated also at higher temperatures. The deviations from the present model range from -0.06 to -0.15 at 7.9 mol $\cdot$ kg^{-1}, and from -0.017 to -0.034 at 5.4 mol $\cdot$ kg^{-1}. Since their results at 3.0 mol $\cdot$ kg^{-1} results are higher then the present values by 0.005 to 0.017, magnifying the correction for more residual water content in their calcium chloride than assumed by the authors [68] would not improve the agreement. It seems likely that other experimental errors have also contributed to these deviations.

Figure 6 shows osmotic coefficients for concentrated CaCl$_2$ from several sources at $T = (323.15$ and $373.15)$ K, including in particular the values tabulated by Smith-Magowan et al. [10] (CODATA tables), the equation of Ananthaswamy and Atkinson [5], and the saturated solution data. The maximum differences between the datasets shown in figure 6 exceed 0.1 at both temperatures, but at $T = 323.15$ K (the top set of curves) there is very good agreement between our model and the model of Ananthaswamy and Atkinson at molalities up to 7.5 mol $\cdot$ kg^{-1}. There is little doubt that the behavior of the model of Ananthaswamy and Atkinson at higher molalities, characterized by a rather sudden turn down, is due to the absence in their database of the saturated-solution data [15,16] and the inclusion of the $T = 323.15$ K results of Jakli and van Hook who reported the high-molality plateau of ϕ at only 2.72 at this temperature. On the other hand, the high-molality values of the osmotic coefficient recommended by CODATA represent an extrapolation of the results of Holmes et al. [7,11] to the saturated-solution data, with a relatively high uncertainty (± 0.14) noted by the authors on the basis of their substantial disagreement with Jakli
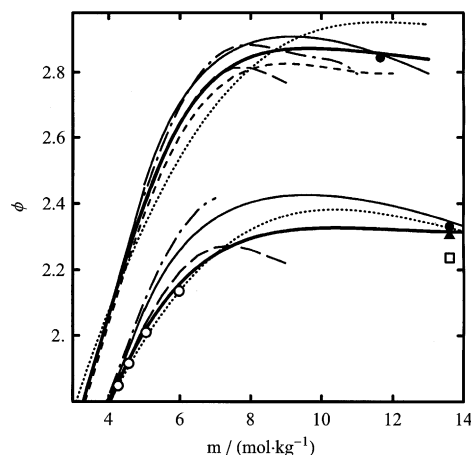
FIGURE 6. Plot of osmotic coefficient of CaCl$_2$(aq) against molality at T = (323.15 and 373.15) K. The higher group of curves corresponds to the lower temperature. —, this work, equation (14); ——, the equation of Pitzer and Oakes [13]; – – –, the equation of Ananthaswamy and Atkinson [5]; —·—, CODATA tables [10]; · · · ··, the equation of Hoffman and Voigt [72]; - - - - - -, isopiestic results of Duckett *et al.* [70] at T = 323.15 K using the LiCl reference standard based on Gibbard and Scatchard [74]; O, isopiestic results of Voigt *et al.* [24] at 373.45 K using the same standard. The remaining symbols represent experimental data at saturation: ●, Collins and Menzies [16]; □ Roozeboom [15]; ▲, author unknown [59].

and van Hook [68]. At T = 373.15 K the difference between osmotic coefficients from references [10,68] at 7 mol · kg^{-1} reaches 0.2 (0.09 · ϕ). However, the later moderately high-molality isopiestic results of Voigt *et al.* [24] at T = 373.45 K, using LiCl as the reference standard, agree very well with our model, even though they were not included in the database due to our initial error in the calculation of the reference data.

Interestingly, the isopiestic results of Duckett *et al.* [70] at T = 323.15 K (see figure 4), reported in a wide molality range from (0.24 to 12) mol · kg^{-1}, with NaCl and LiCl as reference standards, are lower than the present model by about 0.05 in the very high molality region. It should be noted, however, that the shape of their ϕ *vs.* m curve is similar to our model, as shown in figure 4. The excellent agreement of the results of Voigt *et al.* [24] and our preliminary work on the general model for lithium chloride indicate that the equations of Gibbard and Scatchard [74] for LiCl(aq) are not the source of this discrepancy.

Hoffmann and Voigt [72] used a static cell with a thermostated membrane to measure vapor pressures over CaCl$_2$ solutions in a wide range of T = (373.15 to 526) K and m = (3.8 to 25) mol · kg^{-1}. These ranges almost overlap the ranges of the present work, although the measurements were not taken at constant temperatures, but instead at (nearly) constant molalities. Unfortunately, most of the osmotic coefficients calculated from their vapor pressures are higher by about 0.075 (0.02 to 0.11) than the present model, even at 3.8 mol · kg^{-1}, where the uncertainty of earlier and

present results is about ten times smaller. Hoffmann and Voigt also reported coefficients of the extended Pitzer equation with no ionic-strength dependency beyond the second virial, as used by Ananthaswamy and Atkinson [5] for CaCl$_2$ to T = 373 K. As could be expected, this equation was not adequate for much wider ranges of temperature and molality, and the obtained fit was poor. Although the results of Hoffmann and Voigt were not used for parameterization of the current model, the ϕ *vs.* m isotherms at high molality were interpolated directly from the part of their vapor pressure data that was available to us at the time of writing [72]. These isotherms show an extended plateau which can be interpreted as a qualitative corroboration of our model in this region.

The peculiar behavior of the osmotic coefficient of very concentrated CaCl$_2$(aq) has been discussed by Jakli and van Hook [68], Phutela and Pitzer [4], Duckett *et al.* [70], Pitzer and Shi [20], and Pitzer and Oakes [13]. The present work confirms in general the earlier results summarized by Pitzer and Oakes and indicating that the low-temperature maximum changes with increasing temperature to a wider plateau. This plateau, while not as abrupt and flat at lower temperatures as reported by Jakli and van Hook, but wider than indicated by the model of Pitzer and Oakes, is rather difficult to represent using equations based on molality polynomials. Figure 6 shows the essential difference between the present model and the treatment of Pitzer and Oakes, the most general previous representation of the behavior of CaCl$_2$(aq) to very high concentration. Since Pitzer and Oakes did not consider the isopiestic results of Voigt *et al.* [24] (see figure 4) at T = 373.45 K, their equation was based on extrapolation of the model of Holmes *et al.* [11]. The present results reveal that the inflection point in ϕ *vs.* m isotherms lies just above the high molality limit of the latter, so that even a short extrapolation leads to an overestimation of the osmotic coefficients at 5 mol · kg^{-1} and above. As noted in section 1, the association model of Sterner *et al.* [14] reproduces closely the osmotic coefficients obtained from the combination of the models of Holmes *et al.* [11] and Pitzer and Oakes [13].

The same numerical form as for calcium chloride was also used for treatment of calcium bromide data. Only the present results were used in addition to the T = 298.15 K equation of Goldberg and Nutall [73]. A satisfactory fit was obtained using four parameters less, due not only to the much smaller experimental database, but also to a different form of the relationship between osmotic coefficient and molality, more similar to magnesium chloride than to calcium chloride. To the first approximation, the water-activity-lowering capacity of calcium bromide in moderately concentrated solutions is similar to that of calcium chloride at temperatures (80 to 100) K lower. For

example, the osmotic coefficient is 1.80 for 4 $mol \cdot kg^{-1}$ solutions of $CaBr_2$ at $T = 455.75$ K and for $CaCl_2(aq)$ of the same molality at $T = 371.15$ K, a difference of 85 K. Since at lower temperatures the extended plateaus on the osmotic coefficient isotherms for $CaBr_2(aq)$ occur at molalities exceeding the current measurement range, and additionally isopiestic molalities are significantly lower for $CaBr_2$ than for $CaCl_2$, it is easier to achieve a satisfactory model for the former in the same ranges of molality. For this reason it should be expected that a more precise model would not necessarily require more parameters.

3.3. Derived thermal properties

Since there are no reliable enthalpy and heat capacity data available at concentrations above 7.26 $mol \cdot kg^{-1}$, the present model was built without using explicitly any enthalpy and heat capacity data, except for the reliance on the model of Holmes *et al.* [11] at molalities below 4.5 $mol \cdot kg^{-1}$. Therefore, it is interesting to compare the present enthalpy predictions with the few experimental results available at concentrations between

these points. As noted above, replacing the constant α_2 in the extended Pitzer equations [28] with equation (18) made the temperature and molality dependence of the second virial coefficient somewhat more complex, in particular in temperature derivatives such as enthalpies and heat capacities. However, the equations remain reasonably simple to implement for computer calculations. Model equations for enthalpy and heat capacity are derived below.

The thermal properties can be obtained through temperature differentiation of the excess Gibbs free energy. Apparent molar enthalpy $^{\phi}L$ and apparent molar heat capacity $^{\phi}J$ are

$$L_{\phi} = -T^2 \big[\partial(G^E/T)/\partial T \big]_{m,P}, \tag{22}$$

$$J_{\phi} = \big(\partial L_{\phi}/\partial T \big)_{m,P}, \tag{23}$$

where G^E is the excess Gibbs free energy per mole of solute. The quantity G^{Em}, defined as

$$G^{Em} = RT\nu(\ln \gamma_{\pm} - \phi + 1), \tag{24}$$

is more positive than excess Gibbs free energy G^E based on ideal mixing quantities that are proportional to the

TABLE 8
Apparent relative enthalpies L_{ϕ} of $CaCl_2(aq)$ calculated using equation (28) and the parameters from table 3

m (mol · kg^{-1})	T/K = 323.15	T/K = 373.15	T/K = 423.15	T/K = 473.15	T/K = 523.15	T/K = 573.15
0.01	1.366	2.544	4.359	7.515	14.04	32.22
0.1	3.119	6.281	11.08	19.28	36.00	81.93
0.2	3.790	7.733	13.85	24.31	45.54	103.4
0.3	4.298	8.673	15.60	27.50	51.61	116.9
0.4	4.753	9.433	16.94	29.90	56.13	126.9
0.5	5.177	10.11	18.08	31.87	59.78	134.9
0.6	5.575	10.76	19.11	33.58	62.88	141.5
0.8	6.301	11.97	20.96	36.54	68.05	152.3
1.0	6.942	13.14	22.69	39.14	72.39	161.0
1.5	8.295	15.85	26.65	44.82	81.30	178.0
2.0	9.535	18.37	30.29	49.81	88.67	191.3
3.0	12.23	23.21	37.07	58.68	100.9	212.1
4.0	15.19	28.11	43.63	66.77	111.2	228.1
5.0	18.76	33.30	50.09	74.16	119.8	240.7
6.0	23.01	38.66	56.21	80.70	126.9	250.6
7.0	27.38	43.79	61.79	86.44	132.9	258.6
8.0	31.47	48.45	66.77	91.46	138.0	265.5
9.0	35.13	52.61	71.17	95.89	142.5	271.6
10.0	38.38	56.30	75.08	99.80	146.5	277.1
11.0	41.27	59.61	78.56	103.3	150.0	281.9
12.0		62.6	81.70	106.4	153.1	286.3
14.0			87.19	111.7	158.5	293.9
16.0			91.92	116.3	163.0	300.2
18.0				120.3	166.8	305.7
20.0				123.9	170.3	310.5
22.0				127.0	173.4	314.8
24.0				129.6	176.1	318.8
26.0					178.5	322.5
28.0						325.9
30.0						328.8

The unit is $kJ \cdot mol^{-1}$.

logarithm of molecular ratios. In the corresponding equation for G^E, a function of only molality

$$\Omega/(vm)\ln(vm/\Omega + 1), \tag{25}$$

appears instead of the unity in equation (23). Even though the difference between G^E and G^{Em} is not negligible at high molalities (the above function is equal to 0.6 at 30 mol $\cdot$ kg^{-1} for a 2:1 electrolyte), the temperature derivatives in equations (22) and (23) are not affected.

The equation for the molar function G^{Em} consistent with equations (14), (15), and (24) is

$$\frac{G^{Em}}{RT} = -|z_+z_-|2A_\phi/b\ln\left(1+bI^{1/2}\right) + 2\sum_{n=2}^{5}(v_1v_2)^{n/2}V_n m^{n-1}, \tag{26}$$

where

$$V_n = V_{n0}(T) + V_{n1}(T)g(x_n). \tag{27}$$

Note that the extended limiting law term in equation (18-7) of reference [3], which corresponds to the above equation (26), contains the factor of 4 instead of 2, in error.

The equation for L_ϕ is

$$L_\phi = v|z_+z_-|A_L/(2b)\ln\left(1+bI^{1/2}\right) - 2RT^2\sum_{n=2}^{5}(v_1v_2)^{n/2}V_n^L m^{n-1}, \tag{28}$$

where the second virial coefficient ($n = 2$) is

$$V_2^L = V_{20}' + V_{21}'g + V_{21}g'x_2', \tag{29}$$

and the nth virial coefficient V_n^L, for $n \in \{3, 4, 5\}$ is

$$V_n^L = V_{n0}' + V_{n1}'g. \tag{30}$$

The temperature derivatives in equations (29) and (30) are

$$g'(x_2) = 2/x_2^3[\exp(-x_2)\{2 + x_2(2 + x_2)\} - 2], \quad g'(0) = -2/3, \tag{31}$$

$$x_2'(T, I) = -A_{\alpha2\ 1}(T - A_{\alpha2\ 2})^{-2}I^{1/2}, \tag{32}$$

and

$$V_{nj}'(T) = -A_{nj\ 2}T^{-2} + A_{nj\ 3}(650 - T)^{-2} + A_{nj\ 4} + 2A_{nj\ 5}T - 2A_{nj\ 6}T^{-3}. \tag{33}$$

TABLE 9
Differences between the apparent molar heat capacity of the solute and the apparent molar heat capacity of the solute in standard state for CaCl$_2$(aq), $C_{p,\phi} - C_{p,\phi}^\infty$, calculated using equation (34) and the parameters from table 3

m (mol $\cdot$ kg^{-1})	T/K = 323.15	T/K = 373.15	T/K = 423.15	T/K = 473.15	T/K = 523.15	T/K = 573.15
0.01	19.5	28.5	46.4	87.3	206	766
0.1	52.2	76.3	122	225	527	1940
0.2	63.1	96.7	155	287	668	2440
0.3	68.5	109	177	327	758	2760
0.4	72.6	117	192	356	825	2990
0.5	76.6	124	204	379	878	3170
0.6	81.1	130	214	398	921	3330
0.8	91.4	140	230	428	991	3570
1.0	103	150	244	452	1050	3760
1.5	135	175	271	498	1150	4110
2.0	163	198	294	532	1220	4360
3.0	208	238	333	582	1330	4740
4.0	248	275	364	616	1400	5010
5.0	283	304	385	634	1440	5220
6.0	308	323	396	642	1460	5380
7.0	325	335	402	644	1480	5520
8.0	339	345	406	643	1490	5630
9.0	351	352	408	643	1500	5740
10.0	362	359	410	642	1510	5840
11.0	373	365	411	642	1520	5930
12.0		370	412	641	1530	6010
14.0			413	637	1540	6160
16.0			412	632	1550	6280
18.0				627	1560	6390
20.0				622	1560	6490
22.0				622	1570	6580
24.0				627	1580	6660
26.0					1590	6740
28.0						6820
30.0						6900

The unit is J $\cdot$ mol^{-1} $\cdot$ K^{-1}.

The equation for the difference between apparent molar heat capacity of the solute in real solution, J_ϕ or $C_{p,\phi}$, and apparent molar heat capacity of the solute in standard state is

$$C_{p,\phi} - C_{p,\phi}^\infty = v|z_+ z_-|A_J(2b)\ln\left(1 + bI^{1/2}\right) - 2RT^2 \times$$
$$\sum_{n=2}^{5} (v_1 v_2)^{n/2} V_n^J m^{n-1}, \qquad (34)$$

where the second virial coefficient ($n = 2$) is

$$V_2^J = 2T^{-1}V_2^L + V_{20}'' + V_{21}''g + 2V_{21}'g'x_2' +$$
$$V_{21}\left(g''x_2'^2 + g'x_2''\right), \qquad (35)$$

and the nth virial coefficient, V_n^J, $3 \geqslant n \geqslant 5$ is

$$V_n^J = 2T^{-1}V_n^L + V_{n0}'' + V_{n1}''g. \qquad (36)$$

Note that the expression for V_n^L, given by equations (29) and (30), is used in equations (35) and (36), reflecting the way these expressions would be coded for computer calculation.

The second temperature derivatives in equations (35) and (36) are

$$g''(x_2) = 2x_2^{-4}[6 - \exp(-x_2)\{6 + x_2(6 + x_2(3 + x_2))\}],$$
$$g''(0) = 1/2, \qquad (37)$$

$$x_2''(T, I) = 2A_{\alpha2\,1}(T - A_{\alpha2\,2})^{-3}(I)^{1/2}, \qquad (38)$$

and

$$V_{nj}''(T) = 2A_{nj\,2}T^{-3} + 2A_{nj\,3}(650 - T)^{-3} + 2A_{nj\,5} + 6A_{nj\,6}T^{-4}. \qquad (39)$$

The limiting slopes A_L and A_J were calculated using the relations

$$A_L = 4RT^2\left(\partial A_\phi/\partial T\right)_P, \qquad (40)$$

$$A_J = \left(\partial A_L/\partial T\right)_P, \qquad (41)$$

and the correlation of the dielectric constant of water of Archer and Wang [75] using the properties of water calculated from the equation of state of Hill [41].

Tables 8 to 11, analogous to tables 4 to 7, are a convenient reference for comparison of thermal properties with other models and for verification of numerical results. Table 8 contains apparent molar enthalpies calculated from equation (28) for $CaCl_2(aq)$ at even temperatures and molalities. Table 9 contains the values of the difference between apparent molar heat capacity of real solutions and solutions in standard state calculated from equation (34). Tables 10 and 11 list the corresponding values for $CaBr_2(aq)$.

Figure 7 shows the comparison of the molar enthalpies of dilution calculated using the present model as a difference between apparent molar enthalpies at final and initial molalities

$$\Delta_{dil}H_m = L_\phi(m_2) - L_\phi(m_1) \qquad (42)$$

TABLE 10
Apparent relative enthalpies L_ϕ of $CaBr_2(aq)$ calculated using equation (28) and the parameters from table 3

m (mol · kg^{-1})	T/K = 323.15	T/K = 373.15	T/K = 423.15	T/K = 473.15	T/K = 523.15	T/K = 573.15
0.01	1.338	2.520	4.345	7.528	14.14	32.74
0.1	2.975	6.069	10.85	19.16	36.50	85.76
0.2	3.704	7.439	13.38	23.88	46.04	109.6
0.3	4.341	8.364	14.93	26.71	51.89	124.8
0.4	4.952	9.139	16.07	28.71	56.05	135.9
0.5	5.540	9.844	17.02	30.27	59.27	144.8
0.6	6.101	10.51	17.86	31.57	61.89	152.0
0.8	7.129	11.76	19.36	33.73	66.08	163.7
1.0	8.029	12.91	20.74	35.60	69.50	173.0
1.5	9.802	15.40	23.89	39.82	76.67	191.2
2.0	11.16	17.42	26.74	43.83	83.19	206.1
3.0	13.77	20.95	32.07	51.70	95.52	231.4
4.0	16.83	24.81	37.62	59.44	106.6	251.7
5.0	20.40	29.51	43.78	67.07	116.2	267.3
6.0	24.79	35.18	50.57	74.57	124.4	279.0
7.0	29.91	41.54	57.68	81.79	131.4	287.9
8.0	35.28	48.03	64.69	88.61	137.5	295.0
9.0	40.47	54.27	71.34	94.93	143.0	300.9
10.0	45.23	60.04	77.49	100.7	147.9	306.0
11.0	49.47	65.27	83.11	106.0	152.3	310.5
12.0	53.19	69.96	88.19	110.8	156.4	314.5
14.0		77.78	96.87	119.2	163.3	321.5
16.0			103.7	125.9	169.2	327.5
18.0			108.9	131.3	174.1	333.0

The unit is kJ · mol^{-1}.

TABLE 11
Differences between the apparent molar heat capacity of the solute and the apparent molar heat capacity of the solute in standard state for CaBr$_2$(aq), $C_{p,\phi} - C_{p,\phi}^{\infty}$, calculated using equation (34) and the parameters from table 3

m (mol · kg^{-1})	T/K = 323.15	T/K = 373.15	T/K = 423.15	T/K = 473.15	T/K = 523.15	T/K = 573.15
0.01	19.5	28.7	46.7	88.2	209	785
0.1	50.5	75.2	122	231	552	2090
0.2	59.2	92.5	153	293	708	2700
0.3	62.7	101	170	331	809	3110
0.4	65.0	106	181	357	883	3420
0.5	67.2	109	189	376	941	3670
0.6	69.6	111	194	391	988	3890
0.8	75.3	115	202	414	1060	4230
1.0	81.8	119	208	430	1120	4500
1.5	97.4	132	223	464	1230	5020
2.0	108	147	241	495	1320	5410
3.0	111	177	284	559	1460	5990
4.0	113	204	323	610	1560	6400
5.0	128	232	352	641	1620	6700
6.0	153	257	371	653	1650	6910
7.0	181	277	380	650	1650	7060
8.0	208	295	383	639	1640	7180
9.0	234	310	384	626	1630	7270
10.0	259	324	385	612	1610	7350
11.0	284	338	385	599	1600	7420
12.0	308	352	387	588	1580	7480
14.0		381	392	569	1560	7590
16.0			401	558	1540	7690
18.0			414	553	1530	7780

The unit is J · mol^{-1} · K^{-1}.

with the experimental results of Simonson et al. [76] at T = 573.15 K and p = 10.3 MPa for the initial molality m_1 = 7.2589 mol · kg^{-1}. Taking into account that the uncertainty of all available vapor pressure data at this temperature is large, and consequently the model is based primarily on the extrapolation of the present results, the agreement is excellent at higher concentrations. At lower concentrations the present equations rely on the model of Holmes et al. [11] who used enthalpies of dilution and heat capacities only up to 523.15 K. A comparison of the two models up to this temperature shows negligible differences between calculated enthalpies of dilution in the molality range (0.1 to 4.5) mol · kg^{-1}, even though the differences between absolute values of apparent molar enthalpies are noticeable. The deviation from the experimental points at low molality visible in figure 7 indicates that present model could be improved at temperatures above the 523.15 K limit of both the present experimental results and those of Holmes et al. [11] by including the calorimetric measurements of Simonson et al. [76] extending to T = 674 K. This task was postponed until more volumetric and calorimetric results are also available to define the pressure-dependence at high molalities and justify a revision of the low-molality behavior at high temperature. In reference to the validity of figure 7 it should be noted that the pressure effect on the enthalpy

of dilution (the difference between values at pure solvent saturation pressure and at the pressure of the measurements), as estimated from the model of Holmes et al. [11], was negligible at the conditions shown in figure 7. Nevertheless, a pressure-dependent equation is

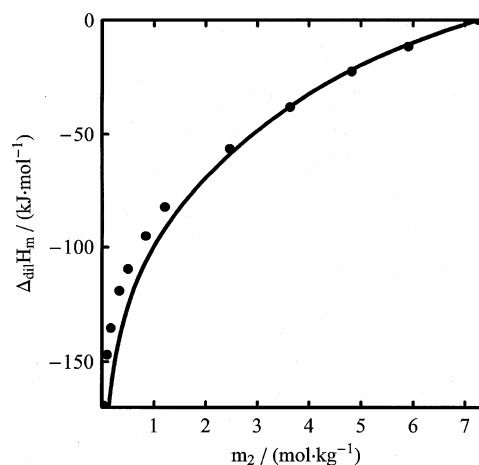FIGURE 7. Plot of enthalpies of dilution against molality at T = 573.15 K for CaCl$_2$(aq). The initial molality was m_1 = 7.2589 mol · kg^{-1}. The enthalpies of dilution are plotted as a function of the final molality m_2. The symbols represent the experimental results of Simonson et al. [76]. The curve was calculated using equation (28) of the present model as $L_{\phi}(m_2) - L_{\phi}(m_1)$.
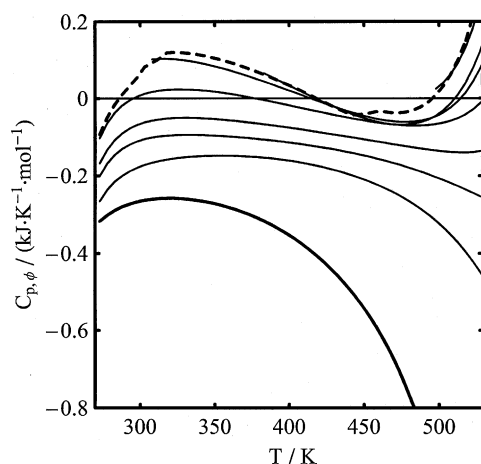
FIGURE 8. Plot of apparent molar heat capacities against temperature for CaCl$_2$(aq) at the molalities (0, 1, 2, 5, 10, 15, 20, 30) mol · kg^{-1} and at the solubility limit. The continuous lines represent constant molalities calculated from the present model using equation (34), and the values in standard state (bold line) from Holmes *et al.* [11]. The dashed line represents approximate values at the solubility limit.

best suited to fully take advantage of high-temperature calorimetric data.

We are not aware of any experimental heat capacity data for CaCl$_2$(aq) at molalities higher than 3.0 mol · kg^{-1} above $T = 348$ K. Figure 8 shows apparent heat capacity $C_{p,\phi}$ calculated from the present model as a function of temperature and molality. The standard state values used for this diagram were taken from Holmes *et al.* and approximated by the following empirical correlation:

$$C_{p,\phi}^{\infty}(T) = -1.892 \cdot 10^7 (\kappa_T / \mathrm{MPa}^{-1})^{1.45}, \tag{43}$$

where κ_T, the isothermal compressibility of the solvent, was calculated using the Hill equation of state [41]. It should be noted that the uncertainty of the difference $C_{p,\phi} - C_{p,\phi}^{\infty}$ calculated from equation (34) is expected to be no less than about 50 J · K^{-1} · mol^{-1}. Additionally, $C_{p,\phi}^{\infty}(T)$, which was obtained effectively by a rather long extrapolation to infinite dilution, introduces an additional uncertainty of at least the same magnitude. Note that the relationship $C_{p,\phi}^{\infty}(T)$ is consistent with the set of parameters obtained by Holmes *et al.* [11], and for this reason their equations are expected to better reproduce the existing experimental heat capacity data below 5 mol · kg^{-1}, even if the present model is equally accurate.

4. Conclusions

The present isopiestic and vapor pressure measurements significantly improve the accuracy of current representations of thermodynamic properties of concentrated aqueous solutions of calcium bromide and calcium chloride. While existing experimental vapor pressure data for calcium chloride covered a wide range of temperature to 673 K and to the solubility limit and above, their accuracy was not sufficient to build a model that could support CaCl$_2$(aq) as an isopiestic reference standard at water activities far below that of saturated sodium chloride. The fraction of previous work that was rejected due to low precision and/ or large systematic errors was larger than expected. Even the present work was affected by an increased uncertainty of vapor pressure measurement at the low temperature limit, due to the defect of the pressure gauges, and an increased uncertainty of concentration at high temperature due to the interference of the small amount of carbon dioxide remaining in the apparatus. Although the present measurements extend to CaCl$_2$ molalities above 20 mol · kg^{-1}, vapor pressures of saturated solutions were not measured in this work, and they remain highly uncertain at temperatures above 420 K for CaCl$_2$(aq) and even more so for CaBr$_2$(aq).

The extremely low solubility product of calcium carbonate in concentrated solutions of CaCl$_2$ is probably the most serious flaw of this electrolyte as a low-water-activity isopiestic reference standard at high temperature. Using CaCl$_2$ as the isopiestic standard for accurate work at water activity below about 0.5 at temperatures above $T = 450$ K requires a very thorough removal of carbon dioxide. Small cells, including those used for vapor pressure measurements, need to have particularly clean and smooth surfaces with low specific surface areas. Degassing the cells at a temperature higher than that of the measurements seems to be necessary. In this aspect lithium chloride might be a better choice for a universal reference standard.

The equations presented here allow for calculation of thermodynamic properties of solutions at the saturation pressure of the solvent. While including calorimetric data would improve the equations at low molality and high temperature, we felt that the amount of existing volumetric and calorimetric data and higher concentrations did not warrant the extension of the work to a more general pressure-dependent model. Even without pressure-dependence, the existing data are not sufficient for regression of a model with even modest extrapolation capability. Due to the combination of complex association and hydration behavior of concentrated calcium chloride solutions, it is difficult to accurately reproduce the correlation between osmotic coefficient and concentration using the virial equation.

The difference between the present model and the earlier equations of Holmes *et al.* [11] in their range of applicability is not significant. Furthermore, the existing $T = 298.15$ K equations [21,28] can be used for ultimate accuracy at this temperature. The improvement in relation to the previous representations
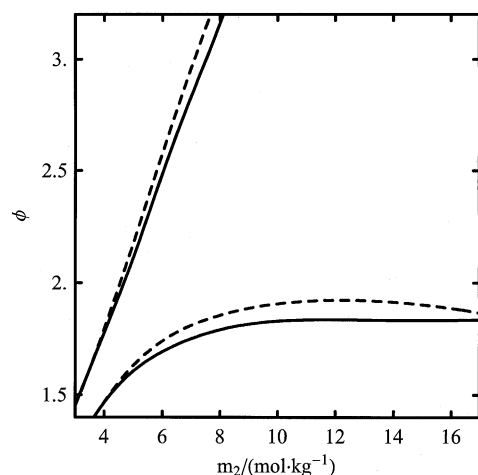
FIGURE 9. Plot of osmotic coefficients against molality at $T = 428.15$ K for $MgCl_2$(aq) (steep lines) and for $CaCl_2$(aq) (flat lines). The isopiestic ratios between the two electrolytes are based on the results of Brendler and Voigt [31]. The continuous lines are based on the present model for $CaCl_2$(aq). The dashed lines are based on the comprehensive model for $MgCl_2$(aq) of Wang *et al.* [6].

of the properties of $CaCl_2$ is the most pronounced at temperatures between (320 and 470) K and at molalities above 5 $mol \cdot kg^{-1}$.

The new data can be used to resolve existing discrepancies and improve the accuracy of the properties of other electrolytes. For example, taking advantage of the high quality of the isopiestic measurements of Brendler and Voigt [31] confirmed by this work, their results at $T = 428.15$ K were used together with the present model to calculate the osmotic coefficient of $MgCl_2$(aq). In figure 9, the curves represent osmotic coefficients for $MgCl_2$ (higher) and $CaCl_2$ (lower) which are interrelated through the isopiestic ratios of Brendler and Voigt [31]. The dashed lines are based on the general treatment of thermodynamic properties of $MgCl_2$(aq) described by Wang *et al.* [6] and based mainly on the vapor pressures of Emons *et al.* [77] in the temperature and molality ranges shown, while the continuous lines are based on the present model for $CaCl_2$(aq). The new values of the osmotic coefficient of $MgCl_2$ at $T = 428.15$ K are lower than the values calculated from the model described by Wang *et al.* [6] by an amount increasing with molality and reaching 0.14 at 8 $mol \cdot kg^{-1}$. Below 4 $mol \cdot kg^{-1}$ the difference is no greater than 0.02.

Acknowledgments

References

[1] R.M. Diamond, J. Am. Chem. Soc. 80 (1958) 4808–4812.
[2] K.S. Pitzer, J. Phys. Chem. 77 (1973) 268–559.
[3] K.S. Pitzer, Thermodynamics, third ed., McGraw-Hill, New York, 1995.
[4] R.C. Phutela, K.S. Pitzer, J. Solution Chem. 12 (1983) 201–207.
[5] J. Ananthaswamy, G. Atkinson, J. Chem. Eng. Data 30 (1985) 120–128.
[6] P. Wang, K.S. Pitzer, J.M. Simonson, J. Phys. Chem. Ref. Data 27 (1998) 971–991.
[7] H.F. Holmes, C.F. Baes Jr., R.E. Mesmer, J. Chem. Thermodyn. 10 (1978) 983–996.
[8] H.F. Holmes, R.E. Mesmer, J. Chem. Thermodyn. 28 (1996) 1325–1358.
[9] P.S.Z. Rogers, Dissertation, Earth Sciences Division, University of California, Berkeley, California, March 1981.
[10] D. Smith-Magovan, D. Garvin, V.B. Parker, R.L. Nutall, B.R. Staples, in: D. Garvin, V.B. Parker, H.J. WhiteJr. (Eds.), CODATA Thermodynamic Tables. Selections for Some Compounds of Calcium and Related Mixtures: A Prototype Set of Tables, Hemisphere, Washington, DC, 1987.
[11] H.F. Holmes, R.H. Busey, J.M. Simonson, R.E. Mesmer, J. Chem. Thermodyn. 26 (1994) 271–298.
[12] H.F. Holmes, J.M. Simonson, R.E. Mesmer, J. Chem. Thermodyn. 29 (1997) 1363–1373.
[13] K.S. Pitzer, C.S. Oakes, J. Chem. Eng. Data 39 (1994) 553–559.
[14] S.M. Sterner, A.R. Felmy, C.S. Oakes, K.S. Pitzer, Int. J. Thermophys. 19 (1998) 761–770.
[15] H.W.B. Roozeboom, Rec. Trav. Chim. Pays-Bas 8 (1889) 1–146, Z. Phys. Chem. 4 (1889) 31–65.
[16] E.M. Collins, A.W.C. Menzies, J. Phys. Chem. 40 (1936) 379–397.
[17] V.A. Ketsko, M.A. Urusova, V.M. Valyashko, Zh. Neorg. Khim. 29 (1984) 2443–2445; Russ. J. Inorg. Chem. 29 (1984) 1398–1399.
[18] V.M. Valyashko, M.A. Urusova, V.A. Ketsko, K.G. Kravchuk, Zh. Neorg. Khim. 32 (1987) 2811–2819; Russ. J. Inorg. Chem. 32 (1987) 1634–1639.
[19] J.A. Rard, R.F. Platford, in: Kenneth S. Pitzer (Ed.), Activity Coefficients in Electrolyte Solutions, second ed., CRC Press, Boca Raton, FL, 1991, pp. 209–277.
[20] K.S. Pitzer, Y. Shi, J. Solution Chem. 22 (1993) 99–105.
[21] J.A. Rard, S.L. Clegg, J. Chem. Eng. Data 42 (1997) 819–849.
[22] K. Grjotheim, W. Voigt, B. Haugsdal, D. Dittrich, Acta Chem. Scand. A 42 (1988) 470–476.
[23] W. Voigt, D. Dittrich, B. Haugsdal, K. Grjotheim, Acta Chem. Scand. 44 (1990) 12–17.
[24] W. Voigt, B. Haugsdal, K. Grjotheim, Acta Chem. Scand. 44 (1990) 311–316.
[25] Th. Fanghänel, K. Grjotheim, Acta Chem. Scand. 44 (1990) 892–895.
[26] Th. Fanghänel, K. Grjotheim, B. Haugsdal, W. Voigt, Acta Chem. Scand. 45 (1991) 30–36.
[27] Th. Fanghänel, K. Grjotheim, W. Voigt, V. Brendler, Acta Chem. Scand. 46 (1992) 423–431.
[28] K.S. Pitzer, P. Wang, J.A. Rard, S.L. Clegg, J. Solution Chem. 28 (1999) 265–282.
[29] H.F. Holmes, C.F. Baes Jr., R.E. Mesmer, J. Chem. Thermodyn. 11 (1979) 1035–1050.
[30] H.F. Holmes, R.E. Mesmer, J. Phys. Chem. 87 (1983) 1242–1255.
[31] V. Brendler, W. Voigt, J. Solution Chem. 23 (1994) 1061–1072.
[32] G. Hefter, P.M. May, S.L. Marshall, J. Cornish, I. Kron, Rev. Sci. Instrum. 68 (1997) 2558–2567.
[33] H.F. Holmes, R.E. Mesmer, J. Chem. Thermodyn. 30 (1998) 311–326.
[34] H.F. Holmes, R.E. Mesmer, J. Chem. Thermodyn. 18 (1986) 263–275.

[35] A.J. Ellis, Am. J. Sci. 261 (1963) 259–267.

[36] T.V. Mozharova, A.F. Zozulya, S.A. Markel, N.G. Tsurko, Russ. J. Inorg. Chem. 28 (1983) 1355–1358; Zh. Neorg. Khim. 28 (1983) 2389–2393.

[37] L.B. Yeatts, W.L. Marshall, J. Phys. Chem. 71 (1967) 2641–2650.

[38] A.R. Felmy, D.A. Dixon, J.R. Rustad, M.J. Mason, L.M. Onishi, J. Chem. Thermodyn. 30 (1998) 1103–1120.

[39] O.I. Martynova, Yu.F. Samoilov, O.K. Smirnov, S.D. Chekhovskaya, Russ. J. Inorg. Chem. 5 (1960) 7–10.

[40] K.S. Pitzer, J.C. Peiper, R.H. Busey, J. Phys. Chem. Ref. Data 13 (1984) 1–102.

[41] P.G. Hill, J. Phys. Chem. Ref. Data 19 (1990) 1233–1274.

[42] D.G. Archer, J. Phys. Chem. Ref. Data 21 (1992) 793–829.

[43] C.S. Oakes, J.M. Simonson, R.J. Bodnar, J. Solution Chem. 24 (1995) 897–916.

[44] P. Novotny, O. Sohnel, J. Chem. Eng. Data 33 (1988) 49–55.

[45] O. Sohnel, P. Novotny, Densities of Aqueous Solutions of Inorganic Substances. Physical Sciences Data Series 22, Elsevier, Amsterdam, 1985.

[46] C.-T. Liu, W.T. Lindsay, J. Solution Chem. 1 (1972) 45–69.

[47] V.P. Mashovets, V.I. Zarembo, M.K. Fedorov, J. Appl. Chem. USSR 46 (1973) 684–686; Zh. Prikl. Khim. 46 (1973) 650–652.

[48] C.-T. Liu, W.T. Lindsay, J. Phys. Chem. 74 (1970) 341–346.

[49] E.R. Gardner, Trans. Faraday Soc. 65 (1969) 91–96.

[50] E.R. Gardner, P.J. Jones, H.J. de Nordwall, Trans. Faraday Soc. 59 (1963) 1994–2000.

[51] L.F. Silvester, K.S. Pitzer, J. Phys. Chem. 81 (1977) 1822–1828.

[52] H.G. McLeod, A.R. Gordon, J. Am. Chem. Soc. 68 (1946) 56–60.

[53] T. Mussini, A. Pagella, J. Chem. Eng. Data 16 (1971) 49–52.

[54] B.R. Staples, R.L. Nutall, J. Phys. Chem. Ref. Data 6 (1977) 385–407.

[55] H.F. Gibbard, S.L. Fong, J. Solution Chem. 4 (1975) 863–872.

[56] C.S. Oakes, R.J. Bodnar, J.M. Simonson, Geochim. Cosmochim. Acta 54 (1990) 603–610.

[57] C.W. Childs, R.F. Platford, Aust. J. Chem. 24 (1971) 2487–2491.

[58] C.W. Platford, J. Chem. Eng. Data 18 (1973) 215–217.

[59] International Critical Tables, vol. III, McGraw-Hill, New York, 1928, p. 367.

[60] M.F. Bechtold, R.F. Newton, J. Am. Chem. Soc. 62 (1940) 1390–1393.

[61] E.P. Perman, T.W. Price, Proc. Roy. Soc. A 72 (1912) 68–85.

[62] W.R. Harrison, E.P. Perman, Trans. Faraday Soc. 23 (1927) 1–22.

[63] T. Sako, T. Hakuta, H. Yoshitome, J. Chem. Eng. Data 30 (1985) 224–228.

[64] J. Baabor, M.A. Gilchrist, E.J. Delgado, J. Chem. Thermodyn. 33 (2001) 405–411.

[65] S.A. Wood, D.A. Crerar, S.L. Brantley, M. Borcsik, Am. J. Sci. 284 (1984) 668–705.

[66] V.I. Zarembo, S.N. Lvov, M.Yu. Matuzenko, Geokhimiya 4 (1980) 610–614.

[67] R. Crovetto, S.N. Lvov, R.H. Wood, J. Chem. Thermodyn. 25 (1994) 127–138.

[68] G. Jakli, W.A. van Hook, J. Chem. Eng. Data 3 (1972) 348–355.

[69] T.M. Davis, L.M. Duckett, C.E. Garvey, J.M. Hollifield, C.S. Patterson, J. Chem. Eng. Data 31 (1986) 54–55.

[70] L.M. Duckett, J.M. Hollifield, C.S. Patterson, J. Chem. Eng. Data 31 (1986) 213–214.

[71] F.P. Hoffmann, Ph.D. Thesis, Bergakademie Freiberg, 1993.

[72] F.P. Hoffmann, W. Voigt, ELDATA: Int. Electron. J. Phys. Chem. Data 2 (1996) 31–36.

[73] R.N. Goldberg, R.L. Nutall, J. Phys. Chem. Ref. Data 7 (1978) 263–310.

[74] H.F. Gibbard Jr., G. Scatchard, J. Chem. Eng. Data 18 (1973) 293–298.

[75] D.G. Archer, P. Wang, J. Phys. Chem. Ref. Data 19 (1990) 371–411.

[76] J.M. Simonson, R.H. Busey, R.E. Mesmer, J. Phys. Chem. 89 (1985) 558–560.

[77] H.H. Emons, W. Voigt, W.F. Wollny, Z. Phys. Chem. (Leipzig) 267 (1986) 1–11.

JCT 04-202